INTERIM REPORT OF RESEARCH ON FULL-SCALE PRESTRESSED PANEL TYPE BRIDGE

by

Eugene Buth, Assistant Research Engineer, TTI

Howard L. Furr, Research Engineer, TTI

and Harry L. Jones, Assistant Research Engineer, TTI

An Interim Technical Progress Report

A Study of Prestressed Panels and Composite Action in Concrete Bridges Made of Prestressed Beams, Prestressed Sub-deck Panels, and Cast-in-place Deck.

Research Study Number 2-5-70-145

Sponsored by
The Texas Highway Department
In Cooperation with the
United States Department of Transportation
Federal Highway Administration

October 1971

Texas Transportation Institute
Texas A&M University
College Station, Texas

Center for Highway Research
The University of Texas
Austin, Texas

Table of Contents

IMPLEMENTATION

The research program originally planned has not been completed and definitive, conclusive results are not available at this time. However, the tests performed to date indicate that the prestressed panel type bridge construction will perform satisfactorily. Two million cycles of design axle load have been applied to the test structure in each of three positions and have not caused any distress.

In view of the fact that the preliminary results have been positive, it is recommended that in-service evaluation of the prestressed panel type bridge construction be continued.

ABSTRACT

One span of a full-scale highway bridge was constructed and subjected to cyclic axle loads at three load positions. The bridge was constructed with four Texas Highway Department Type B prestressed beams, prestressed panels for the lower portion of the deck, and cast-in-place concrete which bonded the prestressed elements together and formed the upper portion of the deck. The pretensioned prestressed panels served as stay-in-place forms for the cast-in-place portion of the deck. They later became an integral part of the structural deck.

Cyclic axle loads of 41.6 kips were applied to the bridge at two locations at midspan and one location at quarterspan to evaluate the performance of this type of bridge construction. Performance was evaluated by determining the response of the bridge to static loads before and after cyclic loading. Beam deflections, beam strains, and slab strains were measured to determine the structure's response. Two million applications of load have been applied in each of the three positions, and no structural distress has occurred.

INTRODUCTION

This paper reports the status and results to date on the theoretical analysis and experimental evaluation of a prestressed panel type bridge deck. The work reported herein was conducted during the second year of the study and was a cooperative effort between the Center for Highway Research at the University of Texas and the Texas Transportation Institute of Texas A&M University. The results of a field study of in-service structures[1]* and a laboratory study of individual panels[2], conducted as a part of this study, have been reported earlier.

A bridge structure of this type consists of conventional prestressed concrete beams, prestressed concrete panels spanning from beam to beam and forming the lower portion of the deck, and the cast-in-place upper portion of the deck. It is desired to design prestressed panel type bridges on the assumptions that (1) composite action exists among the beams, panels, and cast-in-place deck, and (2) transfer and distribution of wheel loads are accomplished at transverse panel butt joints. This study was undertaken to determine if these two assumptions are correct.

A single span, full-scale model of a bridge deck and supporting beams was subjected to cyclic loadings in the laboratory to evaluate the structural details of this type of construction.

---

*Superscript numerals refer to items in the list of references.

FULL-SCALE MODEL TEST BRIDGE AND SLAB SEGMENT

The full-scale test structure consists of two simulated bent caps; four pretensioned, prestressed Texas Highway Department (THD) Type B beams; pretensioned, prestressed panel subdeck; and conventionally reinforced cast-in-place deck. The structure simulates two lanes of a four lane bridge. The deck contains two rows of interior panels and one row of exterior panels and is nomially 23 feet wide and 50 feet long. The panels span between the beams in simple beam action as forms for the cast-in-place concrete. They remain in place to become an integral part of the structural deck. The beams and panels were furnished by commercial fabricators to meet THD specifications. The cast-in-place slab was fabricated to THD specifications by research personnel. No railings or curbs were constructed. A cut-away view illustrating this type of construction is given in Figure 1. The properties of the prestressed elements and other related data are given in Table 1. Dimensions of the elements and details of the reinforcement are given in Figures 2 through 5. The entire structure was constructed on a structural testing slab in the Civil Engineering Laboratory at Balcones Research Center, University of Texas. Figure 6 is a photograph of the complete structure and testing facility.

The structure was designed in accordance with AASHO specifications[4], where applicable, for an HS20-44 loading. A computer program[3] was used to select the reinforcement in the beams. All other design was accomplished by hand calculations. The prestressed panels were designed such that no tensile stresses would develop in them either during construction or under

service loads. The prestressed panels are joined at their ends by the cast-in-place concrete which engages a three-inch extension of prestressing steel over the prestressed beams (Figures 1 and 10). They are joined at the transverse butt joint by the concrete and reinforcing steel placed on top of them. There is no connection between panels, at this butt joint, in the plane of the panels.

Three methods were used for bonding the concrete to the top surface of the prestressed panels. Z-bars, detailed in Figure 8, were used to provide both shear and tensile bond over a selected portion of the deck (Figure 7). In another area, portland cement grout was thoroughly brushed into the rough surfaces of the panels to serve as a bonding agent. The cast-in-place deck was placed over that grout. Over the remainder of the deck, the cast-in-place concrete was bonded only by the action of the cast-in-place concrete and the panels. At selected transverse butt joints, dowel bars were placed on the surface of the panels and extend across the butt joint (Figure 9). They are intended to aid in transferring a wheel load across the panel joint and distributing it in the longitudinal direction of the bridge. Figures 10 through 15 are photographs illustrating the above structural details.

It was also desired to test and evaluate a structure that contained panels corresponding exactly in detail to those used in the IH635 Trinity River high level bridge. For this test, a segment of a structure containing simulated beams and two prestressed panels was constructed. The dimensions of this test article are given in Figure 16. Figure 17 is a photograph of this slab segment. The details of the panels used are given in Figure 18.

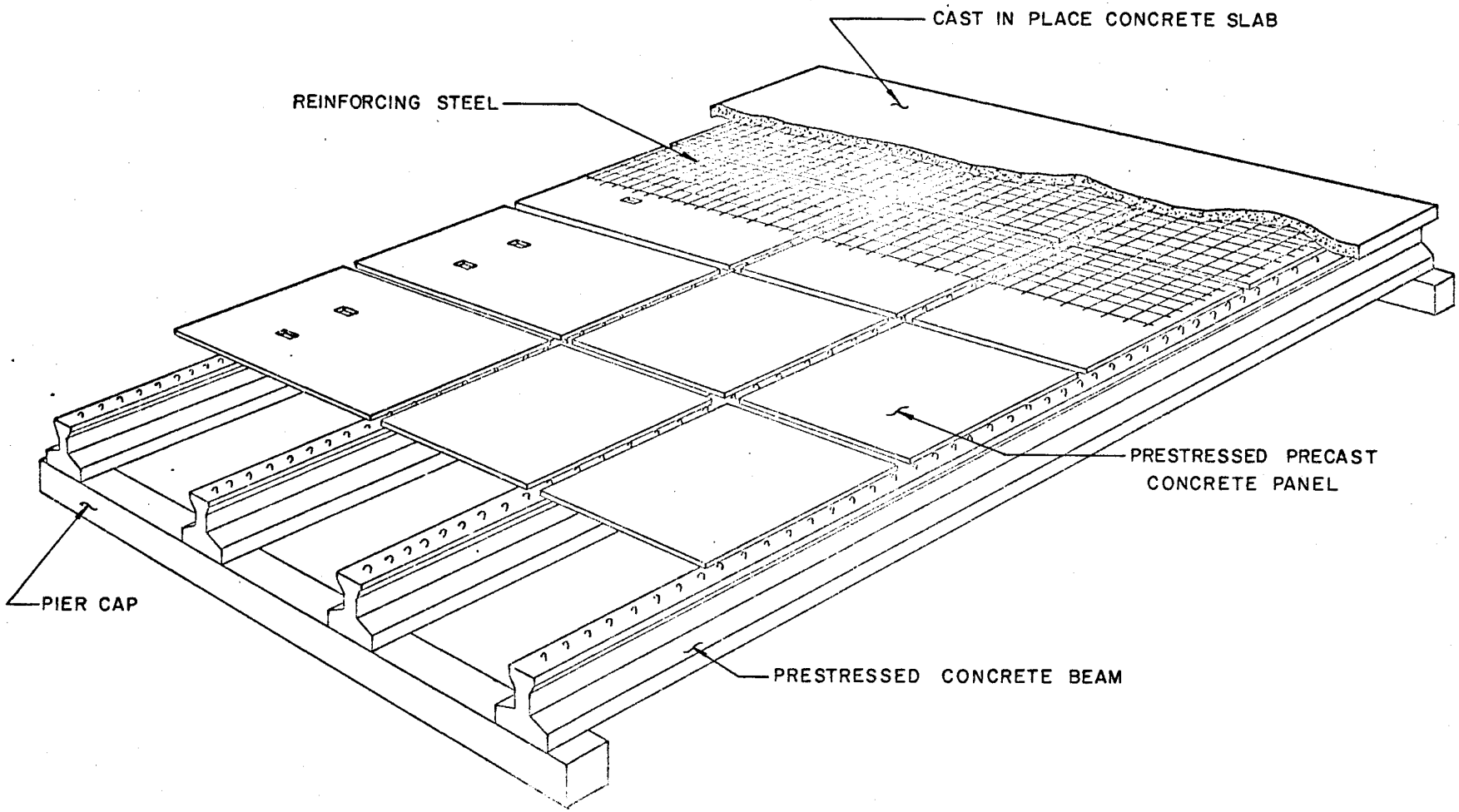

Figure 1. Cut-away view of prestressed panel type bridge.

TABLE 1. CONCRETE STATISTICS

Item	Date Cast	Fabricator	"Release" Strength (psi)	Compressive Strength (psi)	Dynamic Modulus of Elasticity (psi) ASTM C-215
Full-scale Bridge:					
Prestressed Beams	10-29-70 and 10-30-70	Crowe-Gulde Amarillo	4810 4880	7590 @ 28 days and 7130 @ 28 days	6.19×10^6
Prestressed Panels	12-10-70	Span, Inc. Dallas	--	8550 @ 316 days	5.65×10^6
Cast-in-place Deck	2-25-71	TTI	--	5970 @ 240 days	5.23×10^6
Slab Segment:					
Prestressed Panels	8-24-70	Span, Inc. Dallas	4510	6800 @ 7 days	--
Cast-in-place Deck	8-05-71	TTI	--	4400 @ 90 days.	--

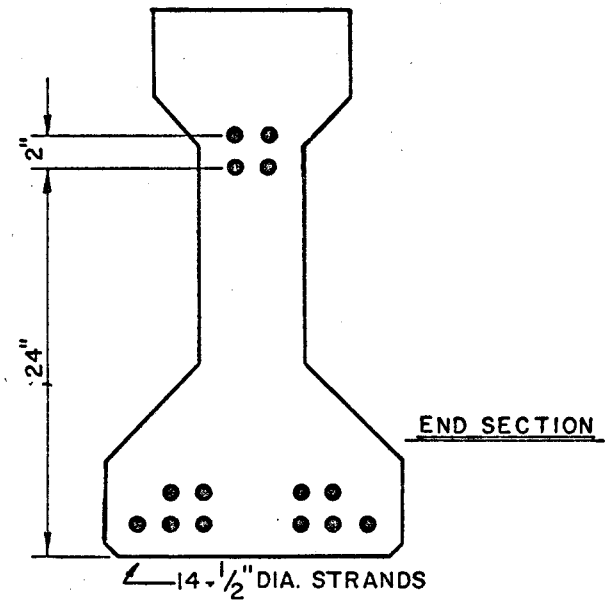

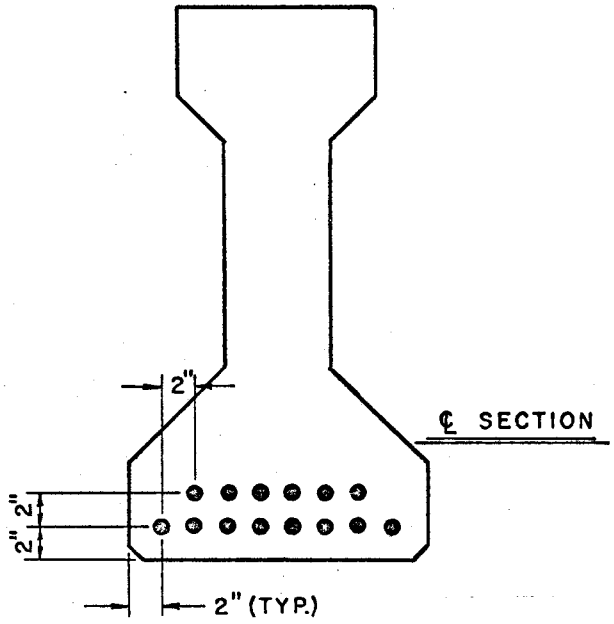

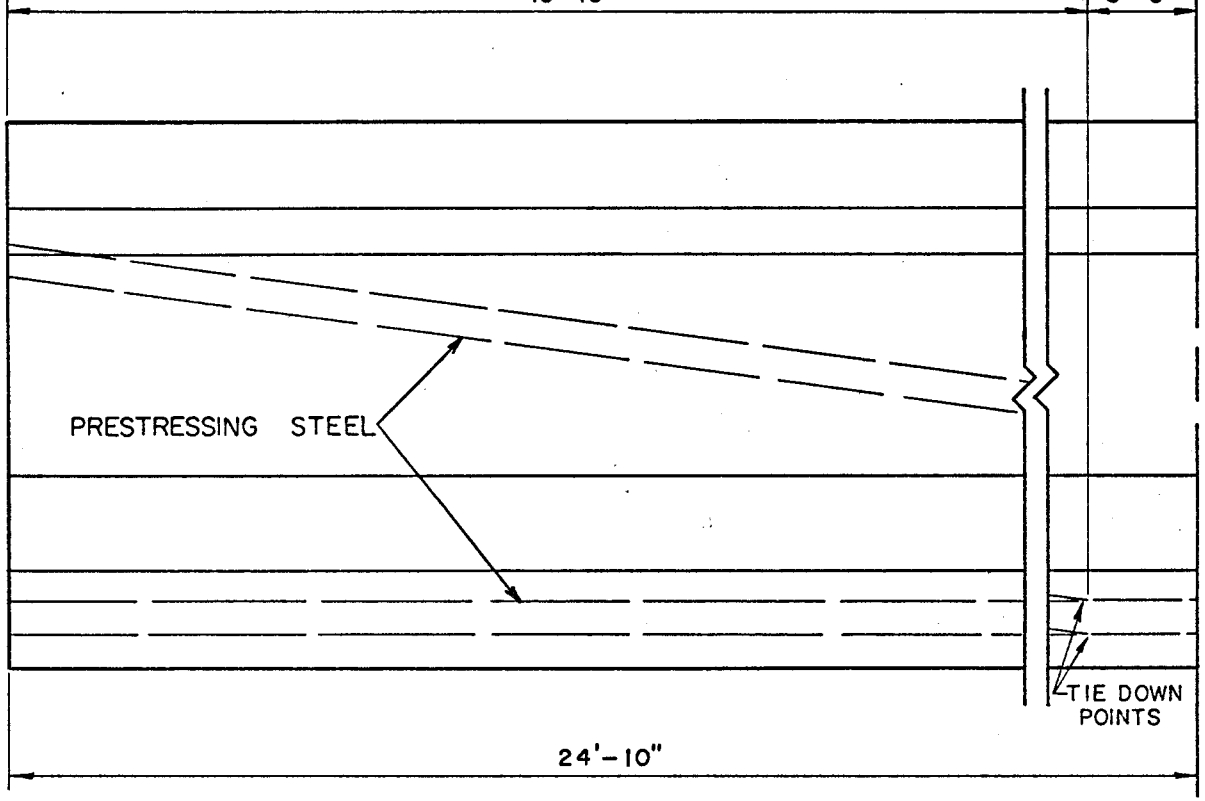

SIDE ELEVATION

SCALE : NONE

Figure 2. Details of prestressing steel in beams.

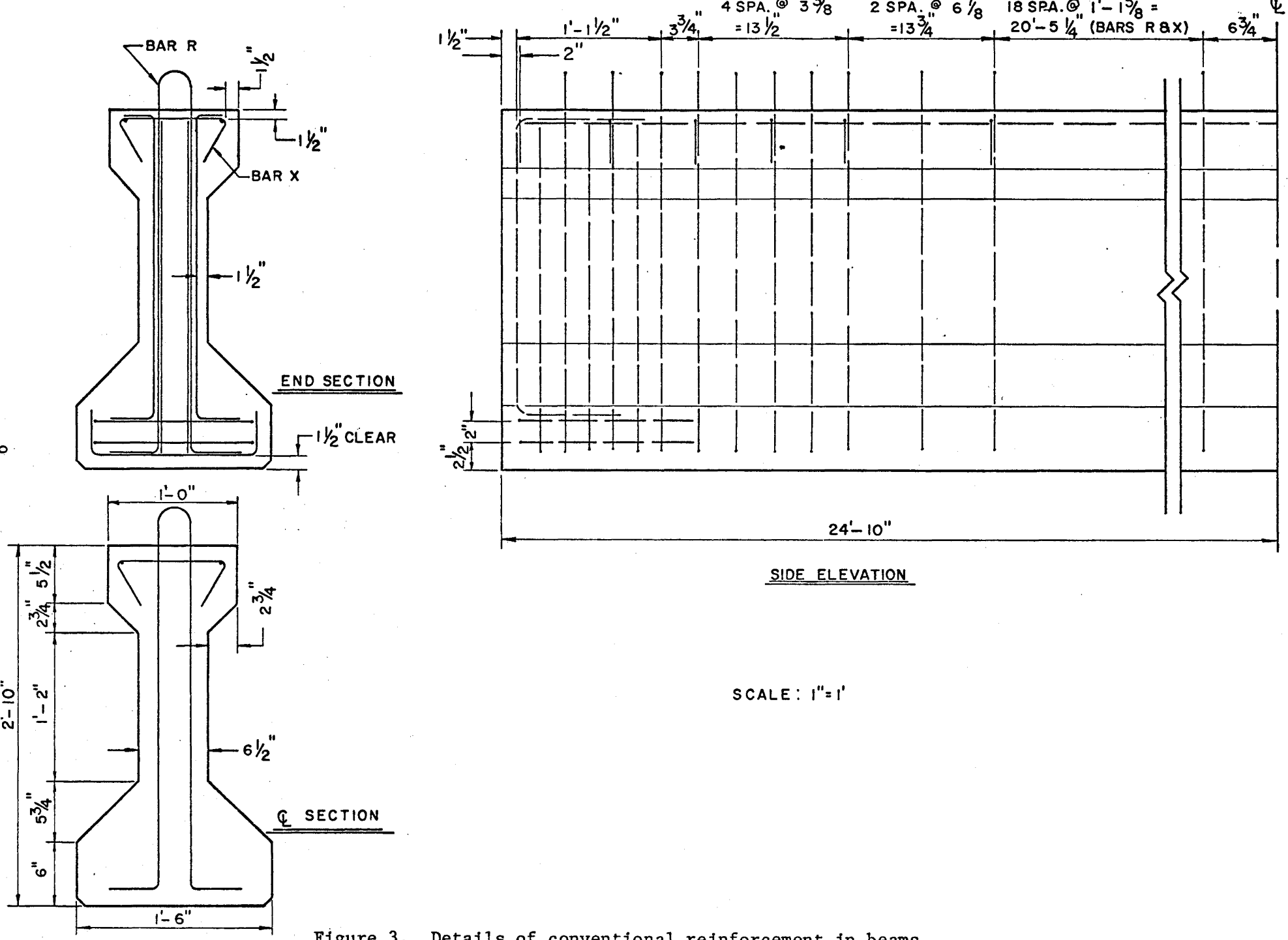

Figure 3. Details of conventional reinforcement in beams.

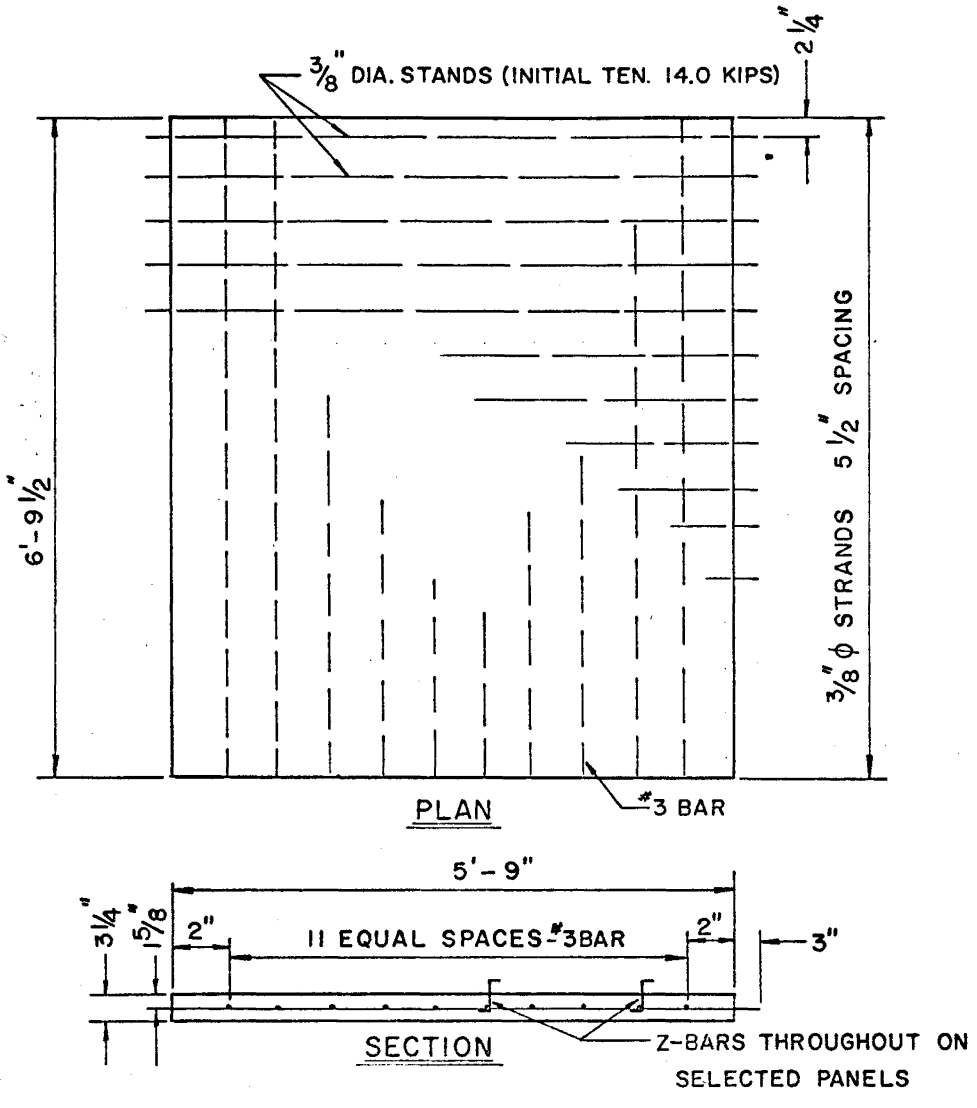

INTERIOR PANEL

Figure 4. Details of interior panels used in full-scale bridge.

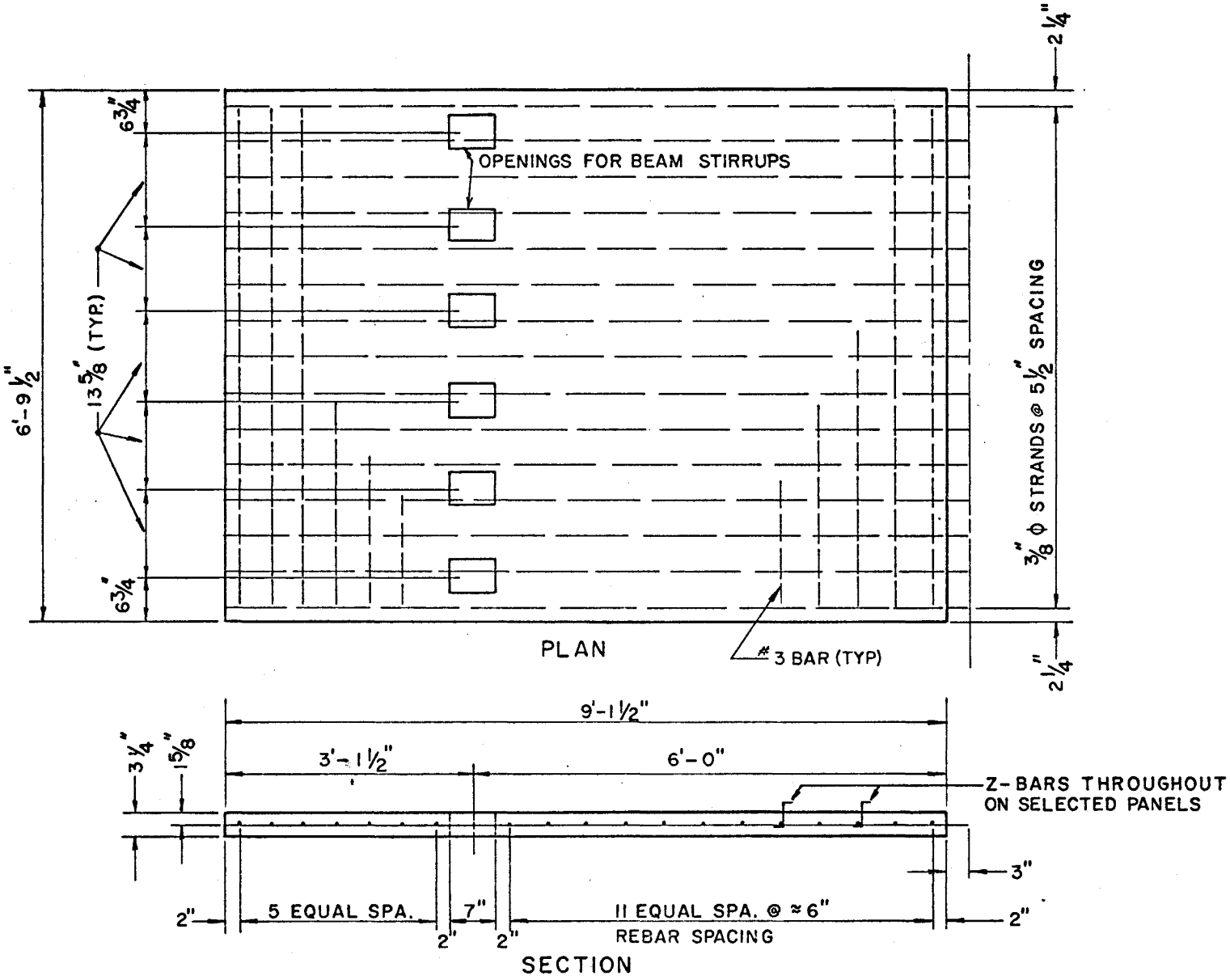

EXTERIOR PANEL

Figure 5. Details of exterior panels used in full-scale bridge.

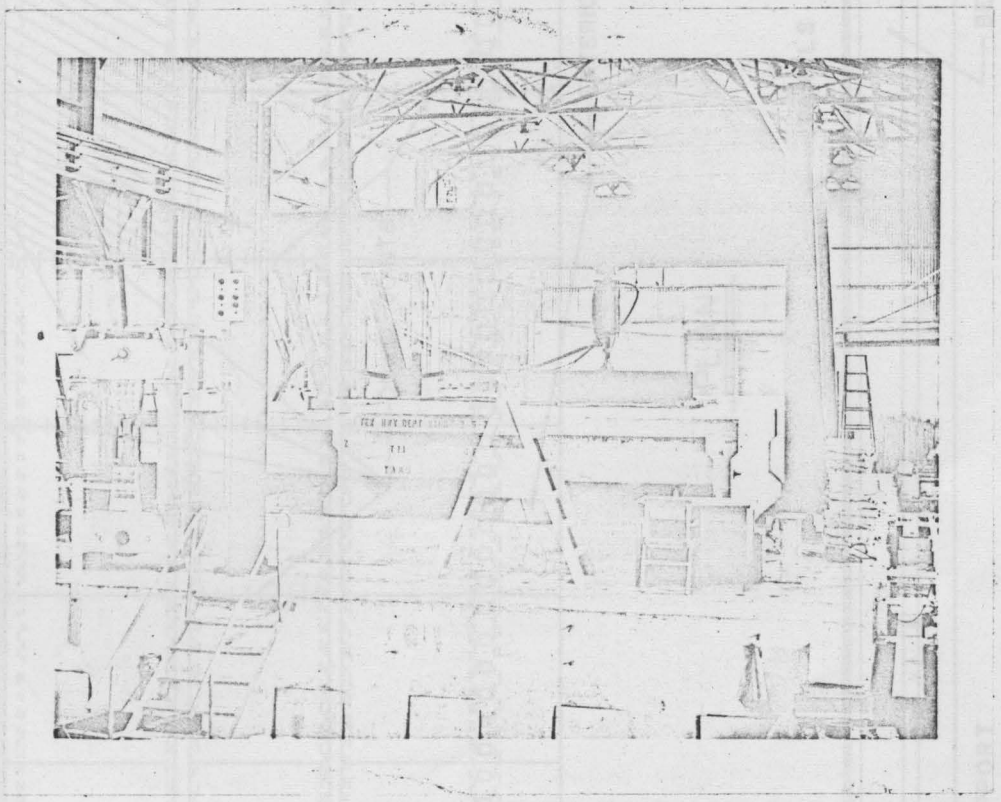

Figure 6. Full-scale model test structure and loading equipment.

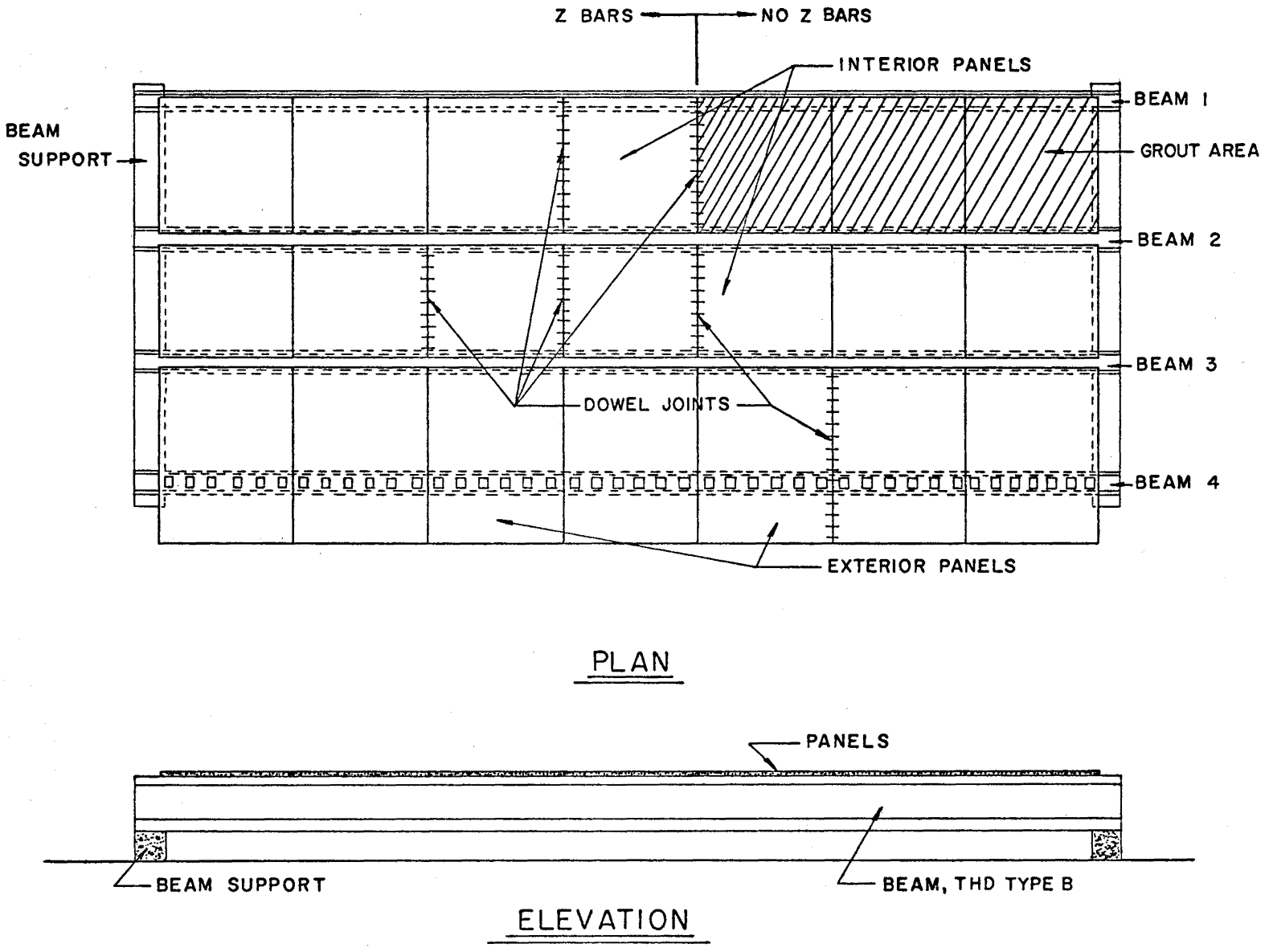

Figure 7. Location and identification of various structural details in full-scale bridge.

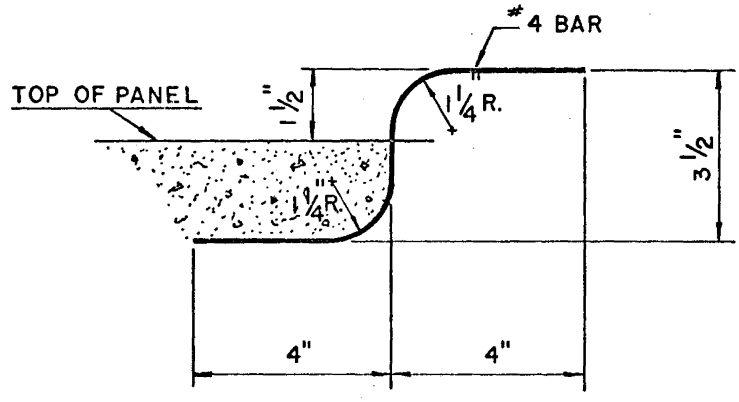

Z BAR DETAIL

Figure 8. Detail of z-bar used in selected panels to aid in providing structural connection between panel and cast-in-place deck.

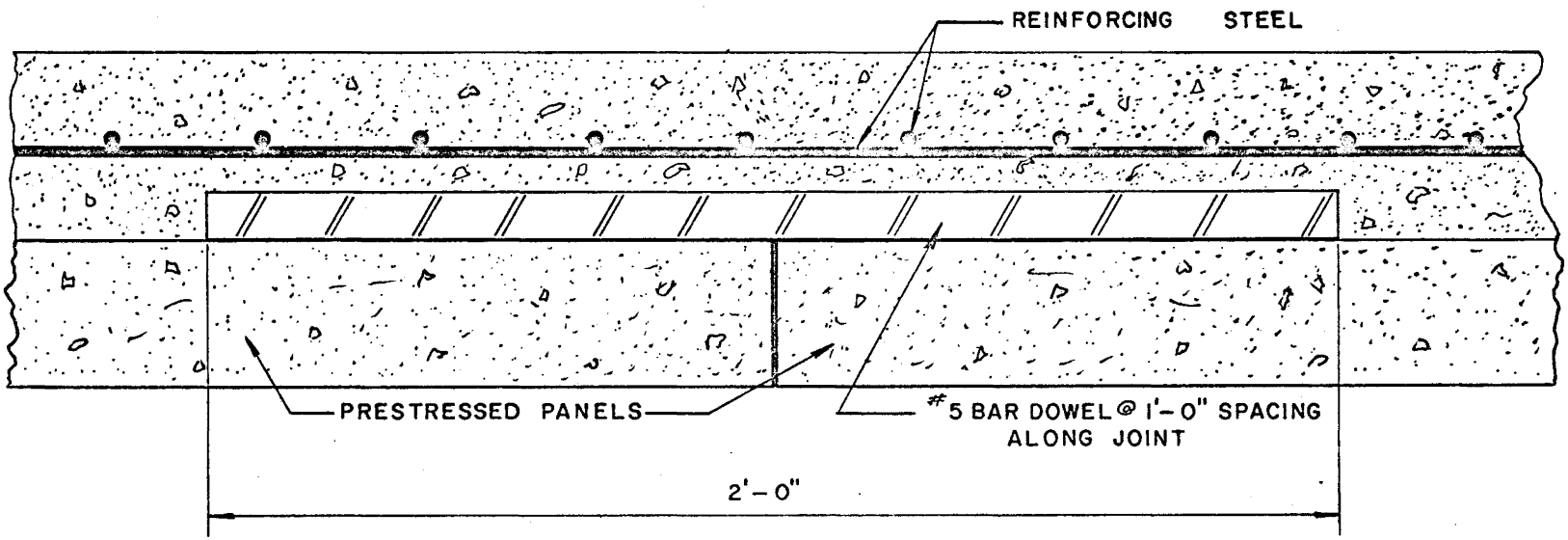

Figure 9. Detail of dowel bar used to aid in transferring and distributing wheel loads across selected panel butt joints.

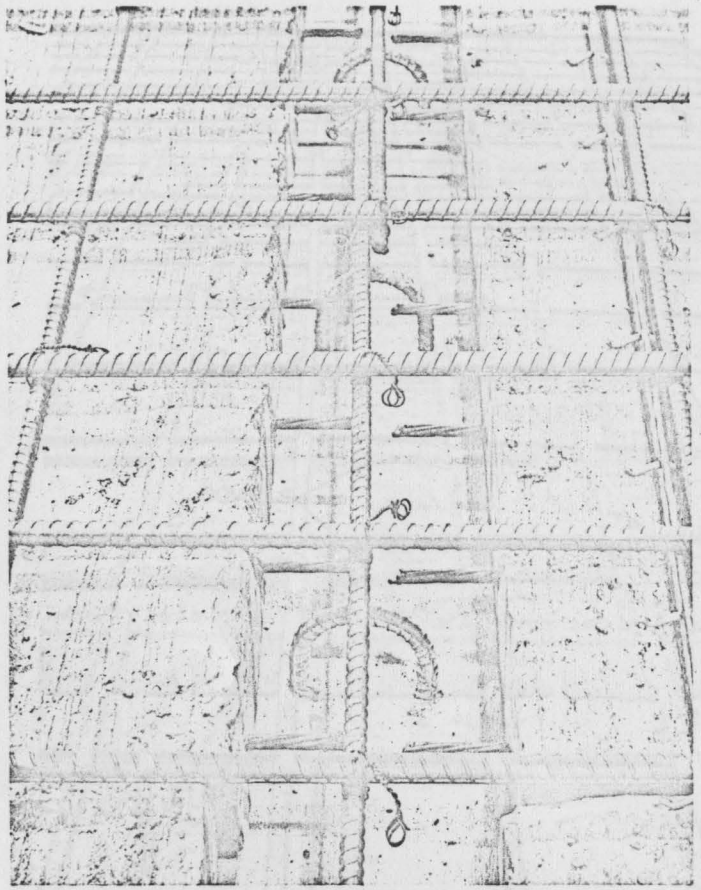

Figure 10. Panel details at interior beam.

Figure 11. Details of exterior panel at exterior beam.

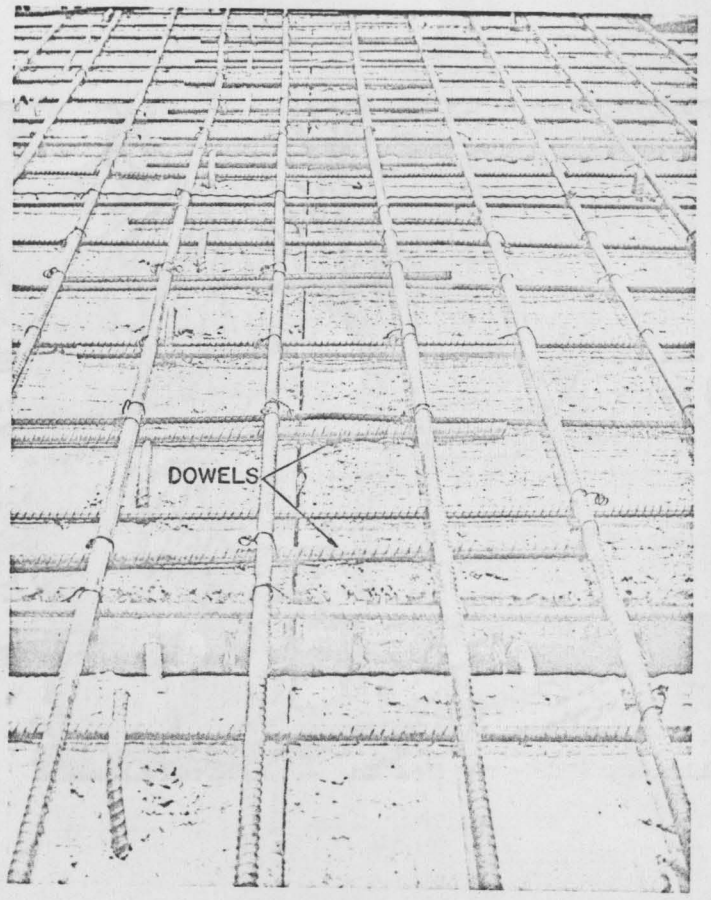

Figure 12. Photo illustrating dowel bars at panel butt joints.

Figure 13. Photo illustrating z-bars.

Figure 14. Concrete being placed on "non-grouted" panel.

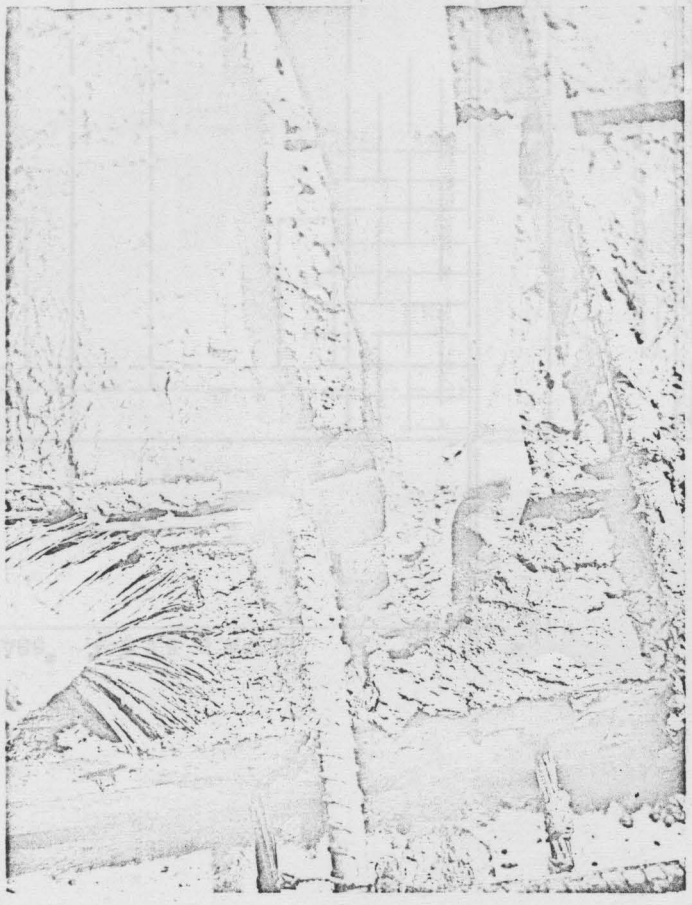

Figure 15. Grout being brushed onto surface of panel.

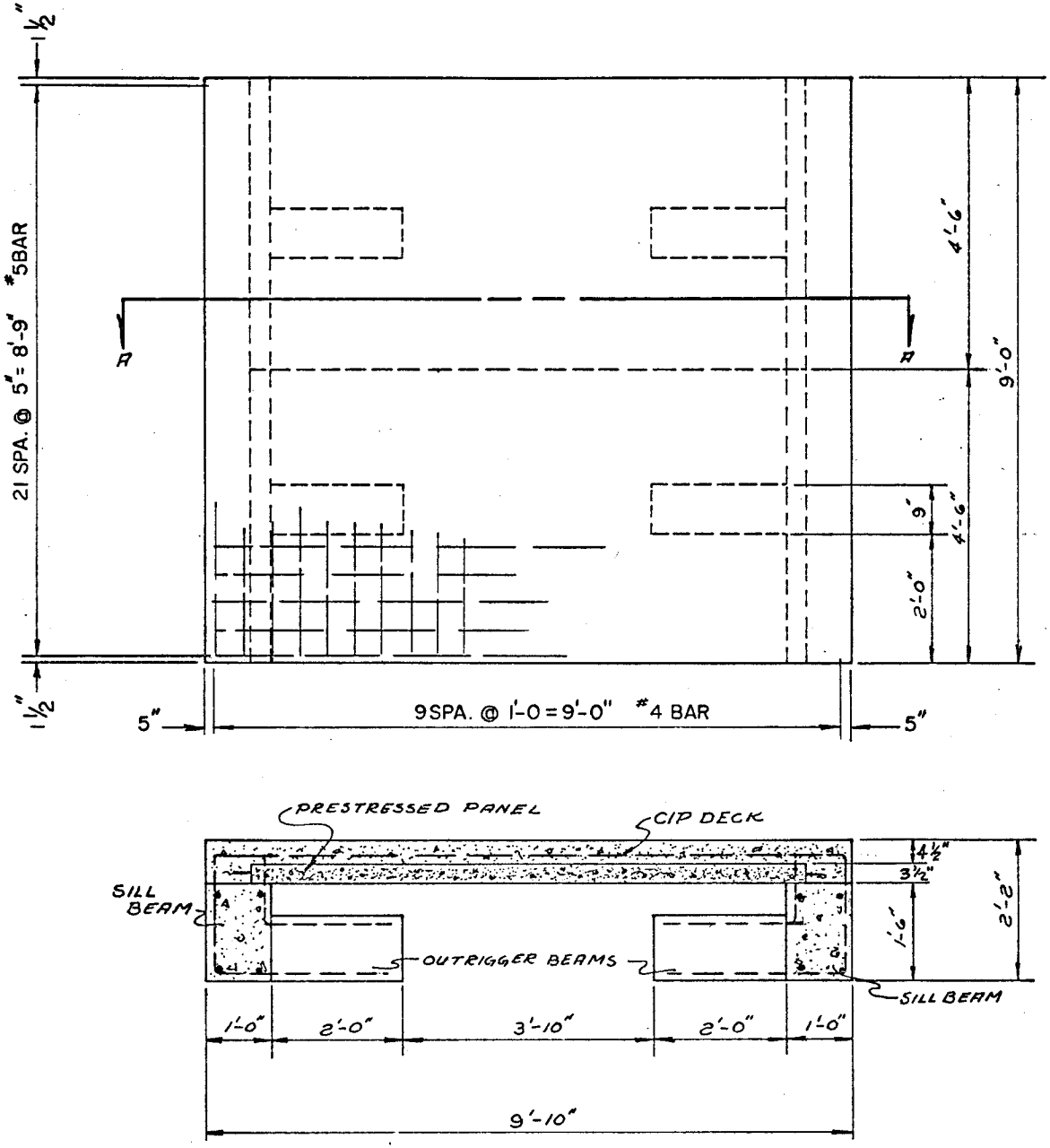

Figure 16. Dimensions and layout of simulated slab segment for loading no. 4.

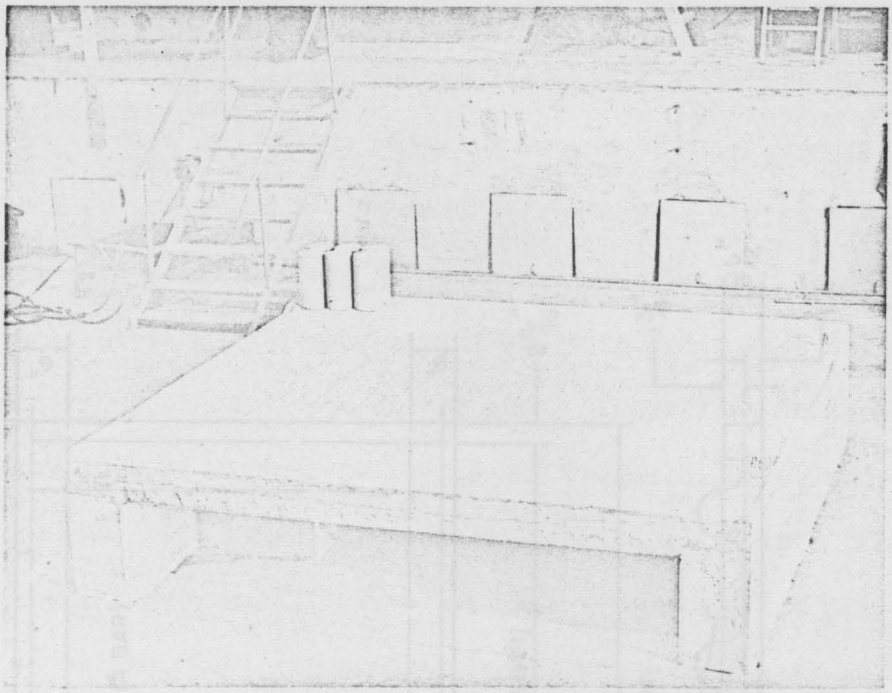

Figure 17. Slab segment for loading no. 4.

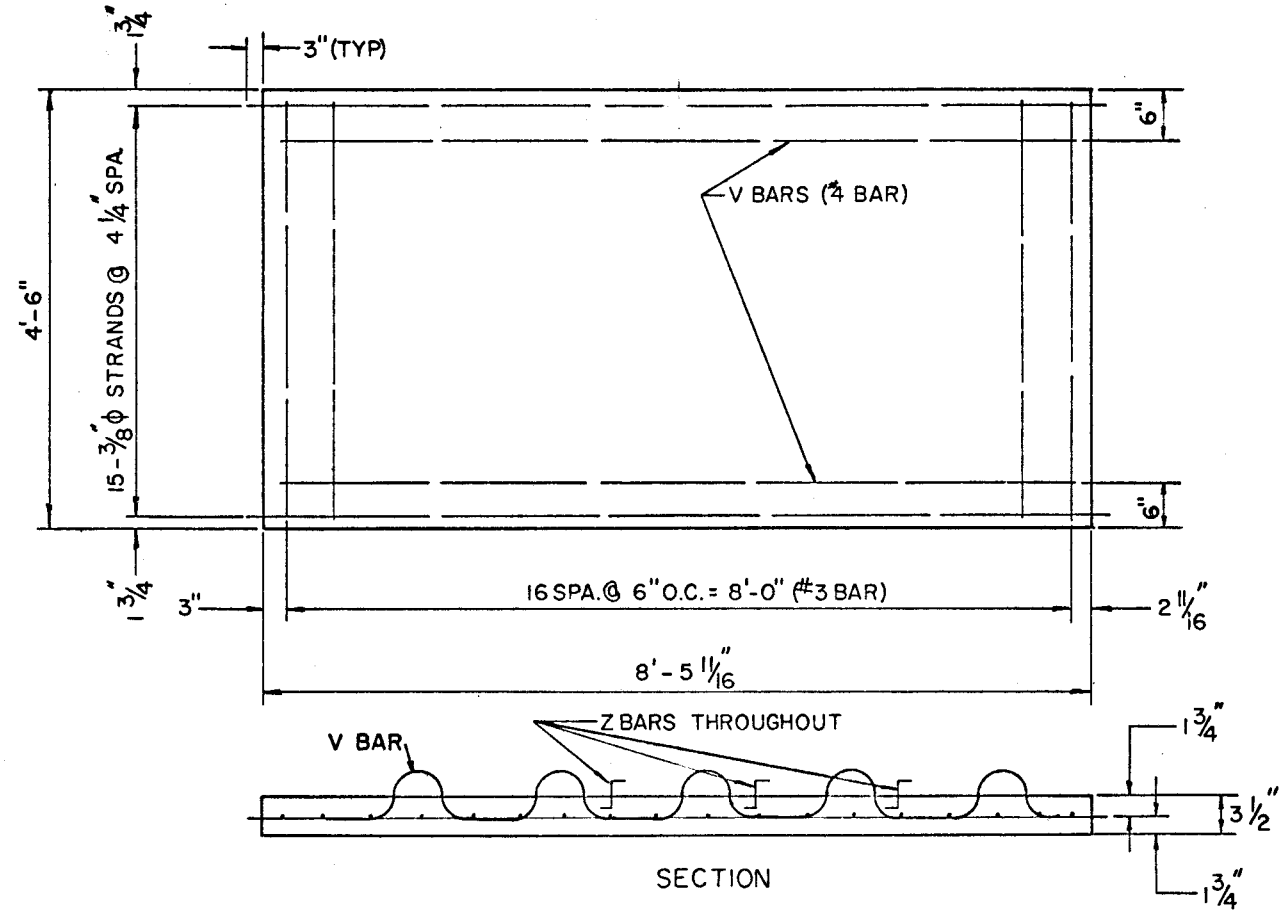

Figure 18. Detail of panels used in slab segment for loading no. 4 (Trinity River Bridge Panel).

INSTRUMENTATION AND LOADING SYSTEMS

The instrumentation layout for the full-scale structure is illustrated in Figures 19 through 22. Gages with the prefix "S" are electrical resistance strain gages and are mounted on the top of the slab and bottom of the prestressed panel and top and bottom of the beams. The slab gages are designed to provide information that would indicate bond failure between slab and panel if such developed at the gage. Leads from these strain gages were connected to a 95-channel switching and balancing unit, and strain readings were made with a manually operated strain indicator. Temperature compensating gages were installed on separate concrete slabs placed above and below the bridge slab. Figures 23 and 24 are photographs of this strain gage system.

Locations indicated with the prefix "D" are linear motion dial gage positions for measurement of beam deflections. The dial gage apparatus illustrated in Figure 25 was used for making these determinations. Information from the beam deflection and beam strain gages enables one to determine if the overall structure maintains its integrity throughout a loading or throughout the entire series of loadings. Deck surface contour measurements were made with dial gages attached to a rigid metal beam as illustrated in Figure 26. This beam was positioned over the points shown in Figure 21.

Linear motion dial gages were also installed to span across panel butt joints in the deck and between the prestressed panels and beams at the positions indicated in Figure 22. The gages across panel butt joints were placed to measure relative vertical displacement of the edges of adjoining panels. Such relative movement would indicate that either a

vertical crack through the cast-in-place slab had developed or that bond at the joint between the panel and cast-in-place slab had failed. Either of these conditions would indicate a local deficiency in the structure. The panel-to-beam gages were placed to measure relative horizontal movement of the two elements in the directions of the longitudinal and transverse axes of the bridge. Any relative movement that might be detected between these elements would indicate slippage resulting from failure of the bond between them.

Two types of loading arrangements are used to simulate loads due to traffic. They are axle loads, loads 1 through 3 in Table 2, and wheel loads, loads 4 through 8. Simulation of axle loads is accomplished with the hydraulic ram and loading pad arrangement illustrated in Figures 27 and 28. The two pads representing the dual wheels of a single heavy axle of a design H20 truck are 12 inches by 20 inches in plan and spaced 6 feet on centers. A Riehle-Los hydraulic testing machine, illustrated in Figure 29, operates the ram for both the static and dynamic axle loadings. The cyclic loading capability of this equipment is derived from a piston and flywheel arrangement driven by an electric motor. The system results in a nearly sinusodial loading for these particular tests (Figure 31). Pressure gages, Figure 30, in the jacking system were calibrated by means of a calibrated load cell set between the jack and the loading plate. Prior to loading in each load position, both static and cyclic load calibrations were made. Simulation of a wheel load rolling across a transverse butt joint between prestressed panels is accomplished with two hydraulic rams acting on loading pads positioned on opposite sides of and adjacent to the transverse joint. The load alternates between the two rams, and one ram loads and unloads

while the other remains inactive. The pulsator used to produce this alternating wheel loading produces a trapezoidal load-time trace (Figure 32).

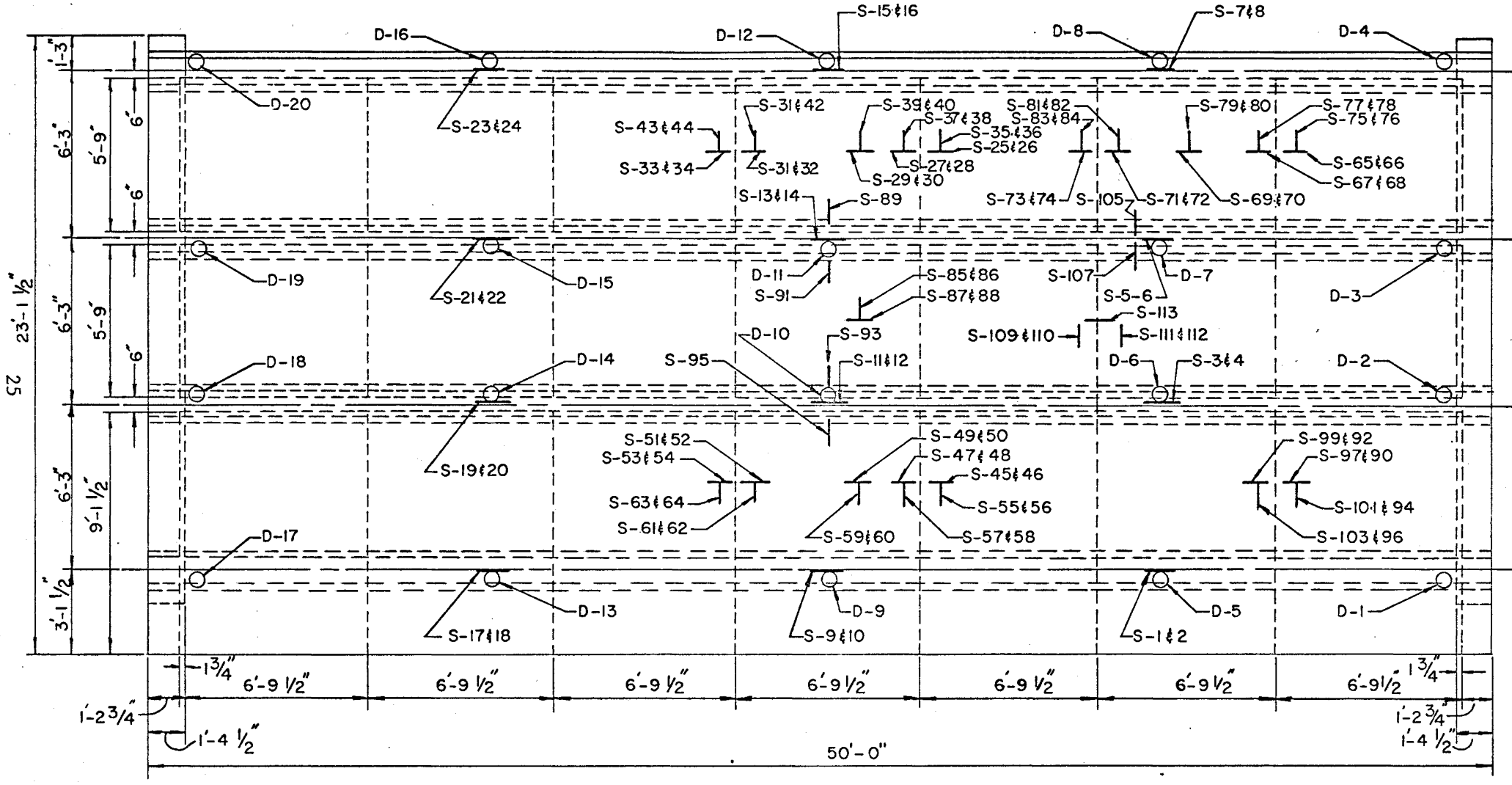

Figure 19. Layout of electrical resistance and beam deflection gages on full-scale bridge. Odd numbered strain gages are on top.

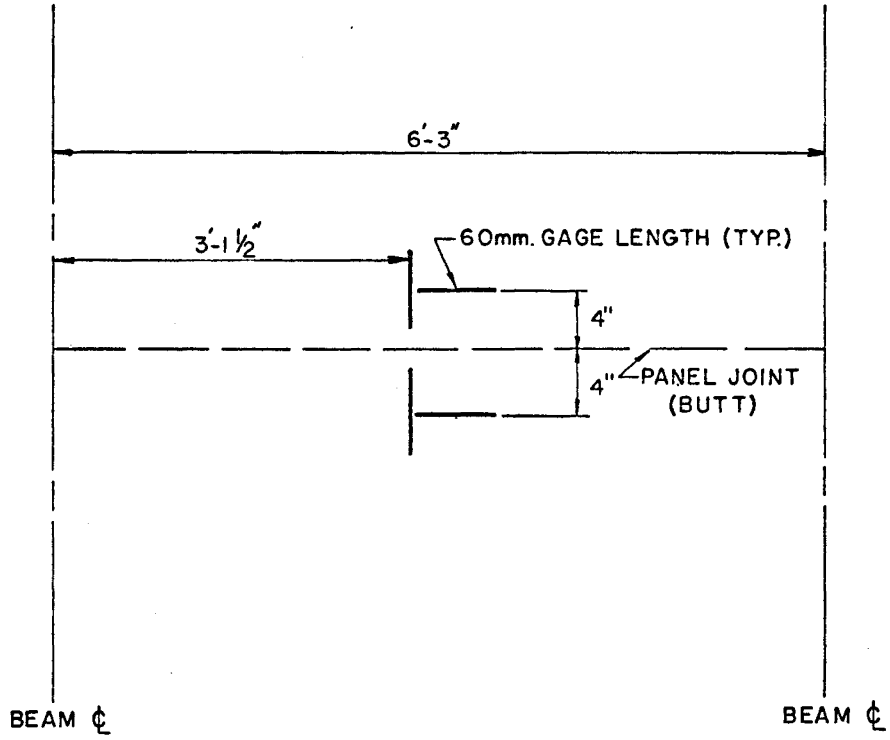

Fig. 20. Typical electrical resistance strain gage pattern on top of slab and bottom of panel at panel butt joint.

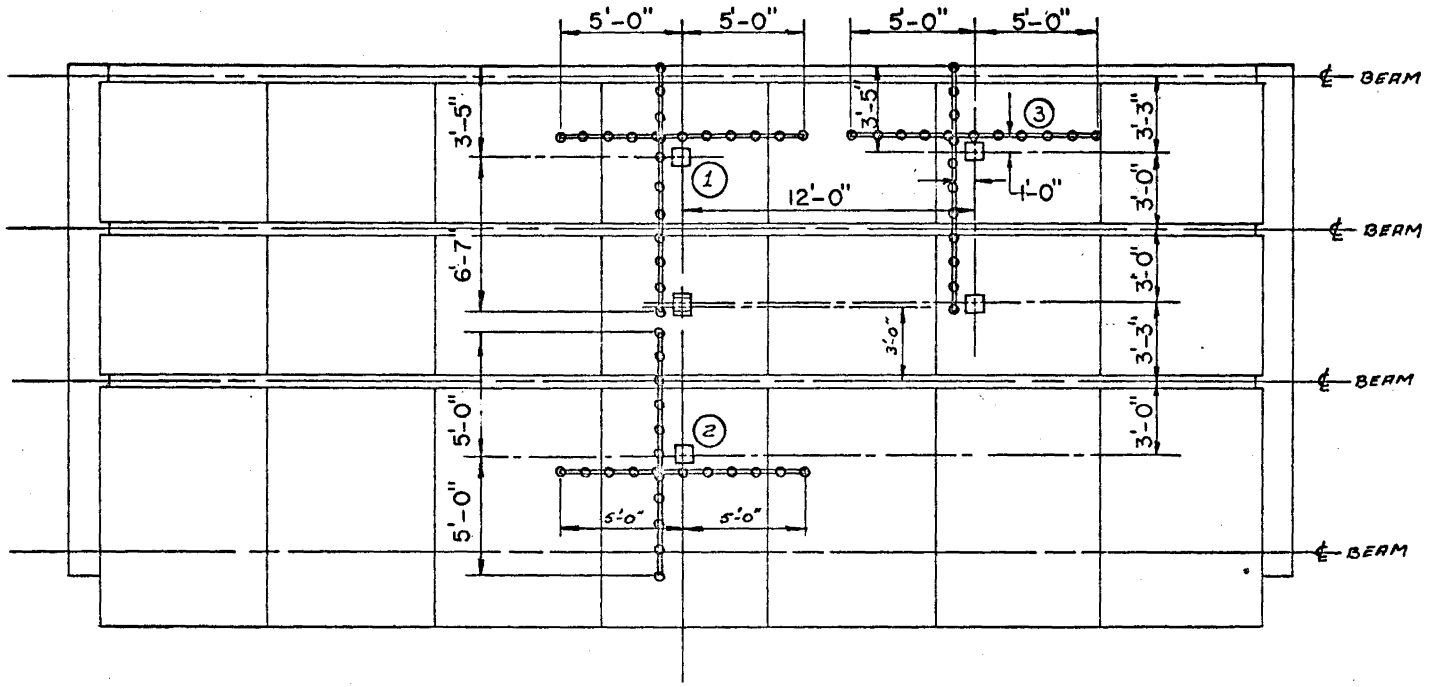

Figure 21. Bridge slab surface contour gage positions for loadings 1, 2, and 3

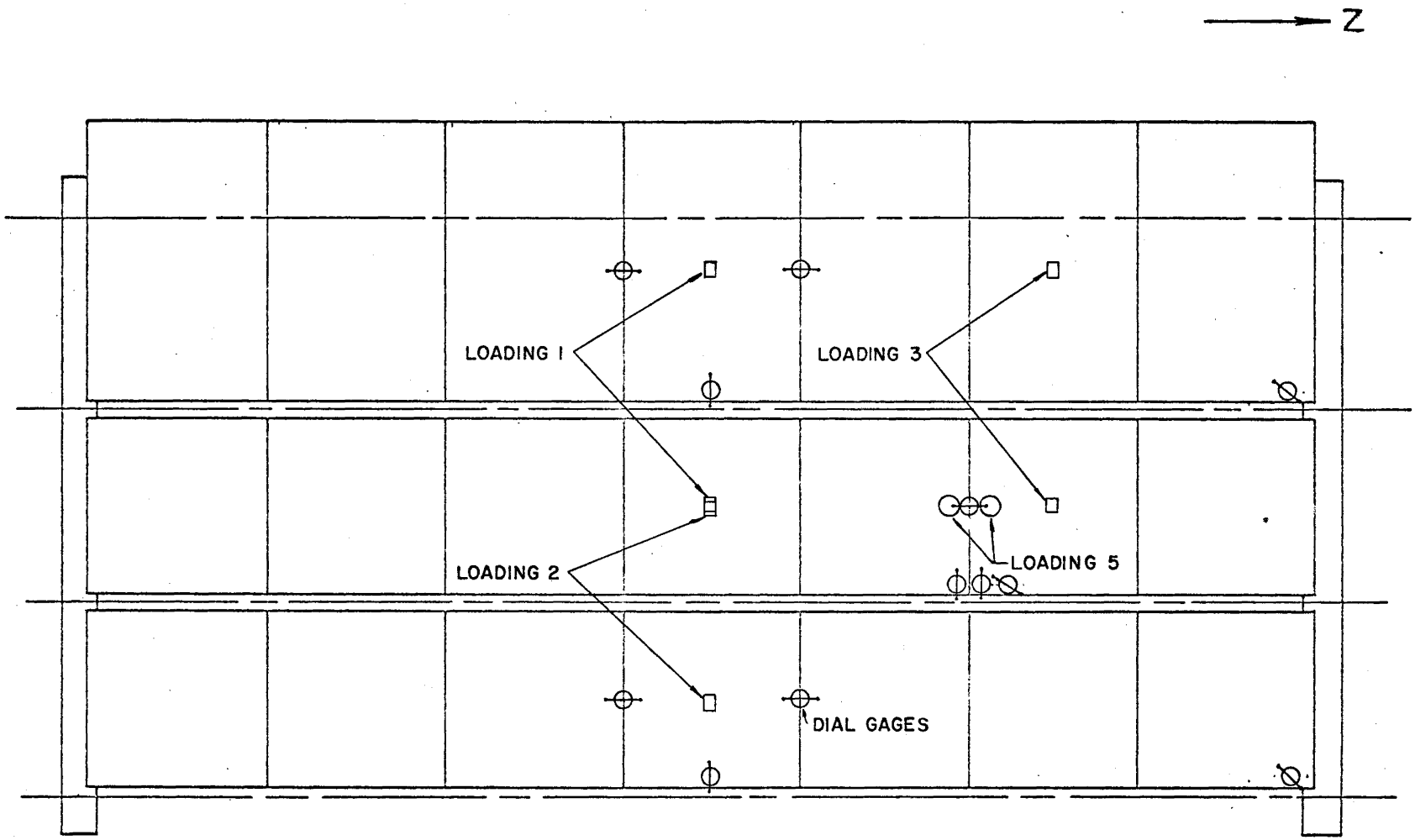

Figure 22. Gage positions for panel-to-panel and panel-to-beam relative displacement dial gages.

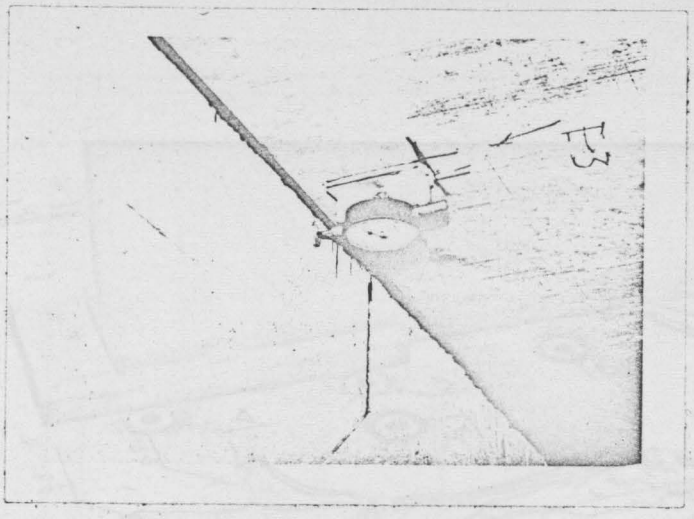

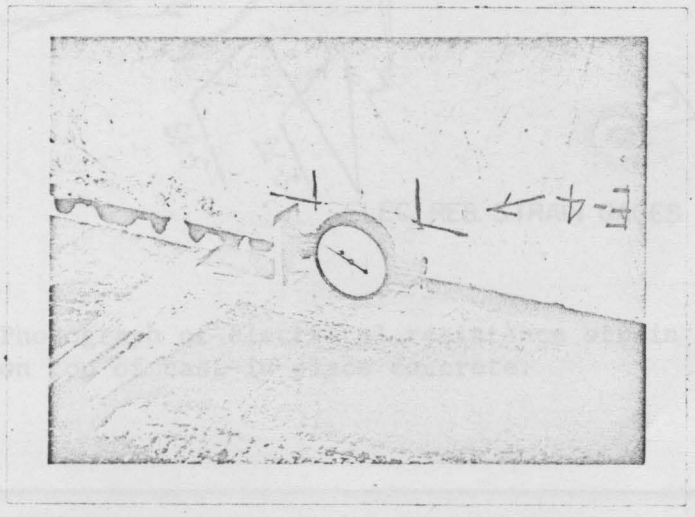

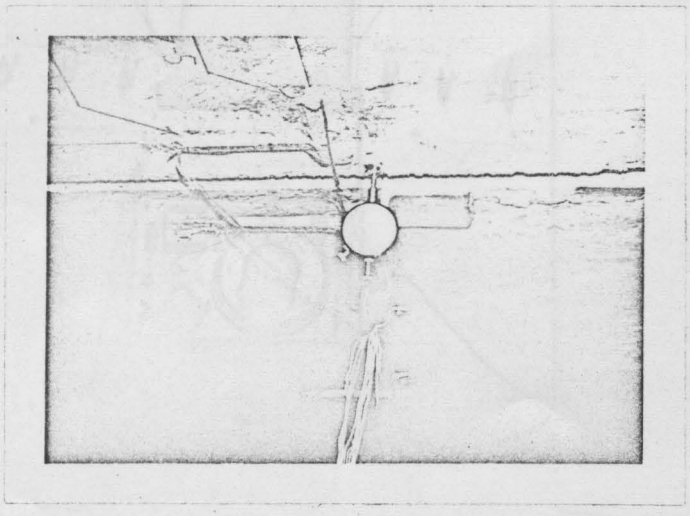

Figure 22a. Linear motion dial gages for detecting relative displacements between panel and beam and between adjoining panels.

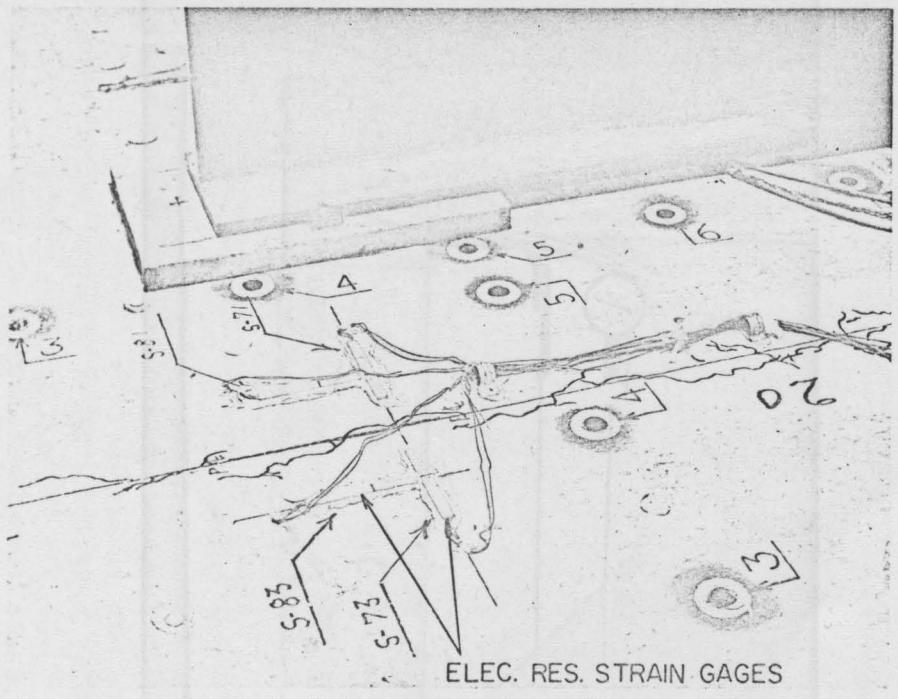

Figure 23. Photograph of electrical resistance strain gage pattern on top of cast-in-place concrete.

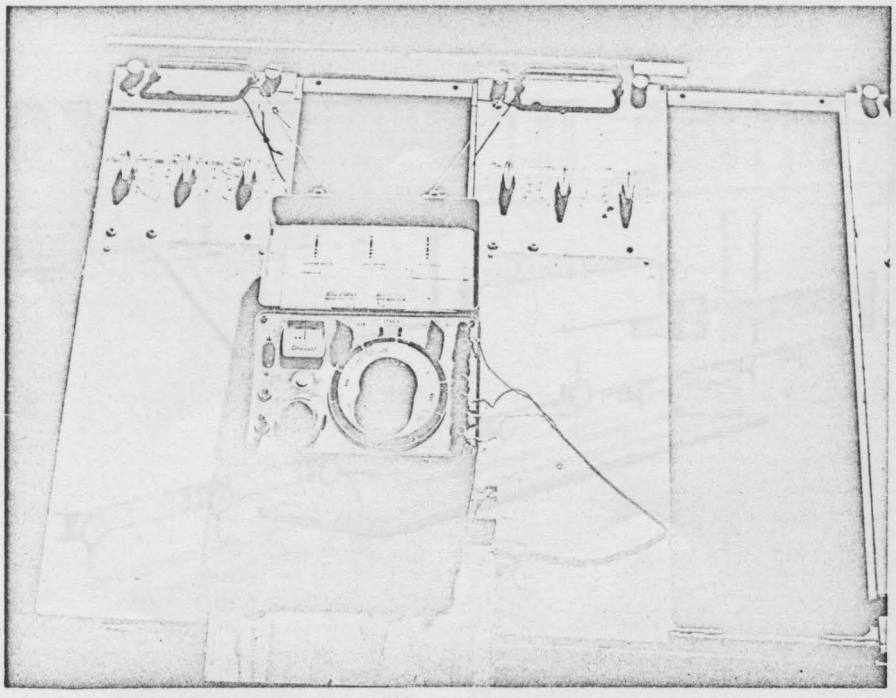

Figure 24. Photograph of electrical resistance strain gage switching and balancing unit and readout unit.

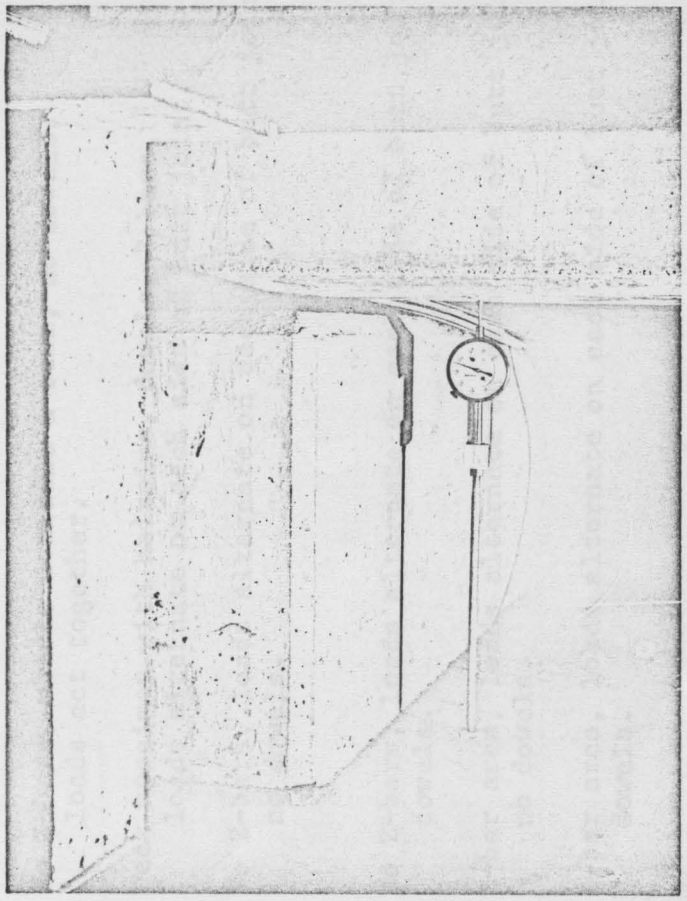

Figure 25. Gage for measuring beam deflection.

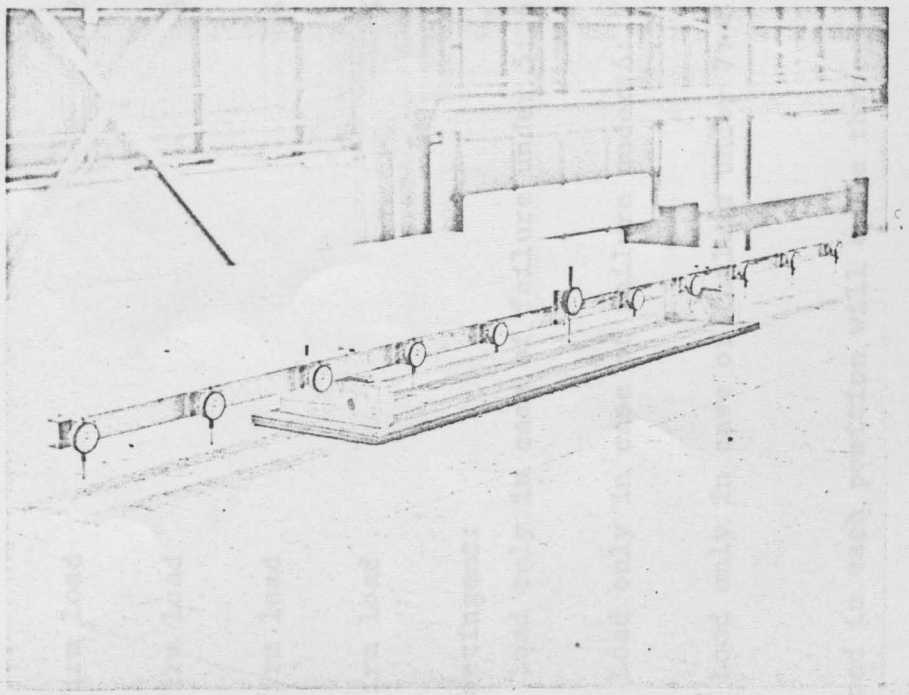

Figure 26. Gages for measuring deck surface contour,

TABLE 2. LISTING OF LOADS

Condition	Load	Type	Remarks
Firm load	1	Axle	Z-bar area, wheels straddle a beam, dowels on each side, loads act together.
Firm load	2	Axle	Z-bar area, wheels straddle a beam, no dowels, loads act together.
Firm load	3	Axle	No Z-bars, wheels straddle a beam, no dowels, loads act together.
Firm load	4	Wheel	Deck specimen with hairpins, dowels, Z-bars, loads alternate on each side of butt joint.
Firm load	5	Wheel	No Z-bars, loads alternate on each side of butt joint, no dowels.
Contingent:			
Load only in case of failure under 5:	6	Wheel	No Z-bars, loads alternate on each side of butt joint, dowels.
Load only in case of failure under 6:	7	Wheel	Z-bar area, loads alternate on each side of butt joint, no dowels.
Load only in case of failure under 7:	8	Wheel	Z-bar area, loads alternate on each side of butt joint, dowels.

Load in each position will cycle through 2,000,000 applications.

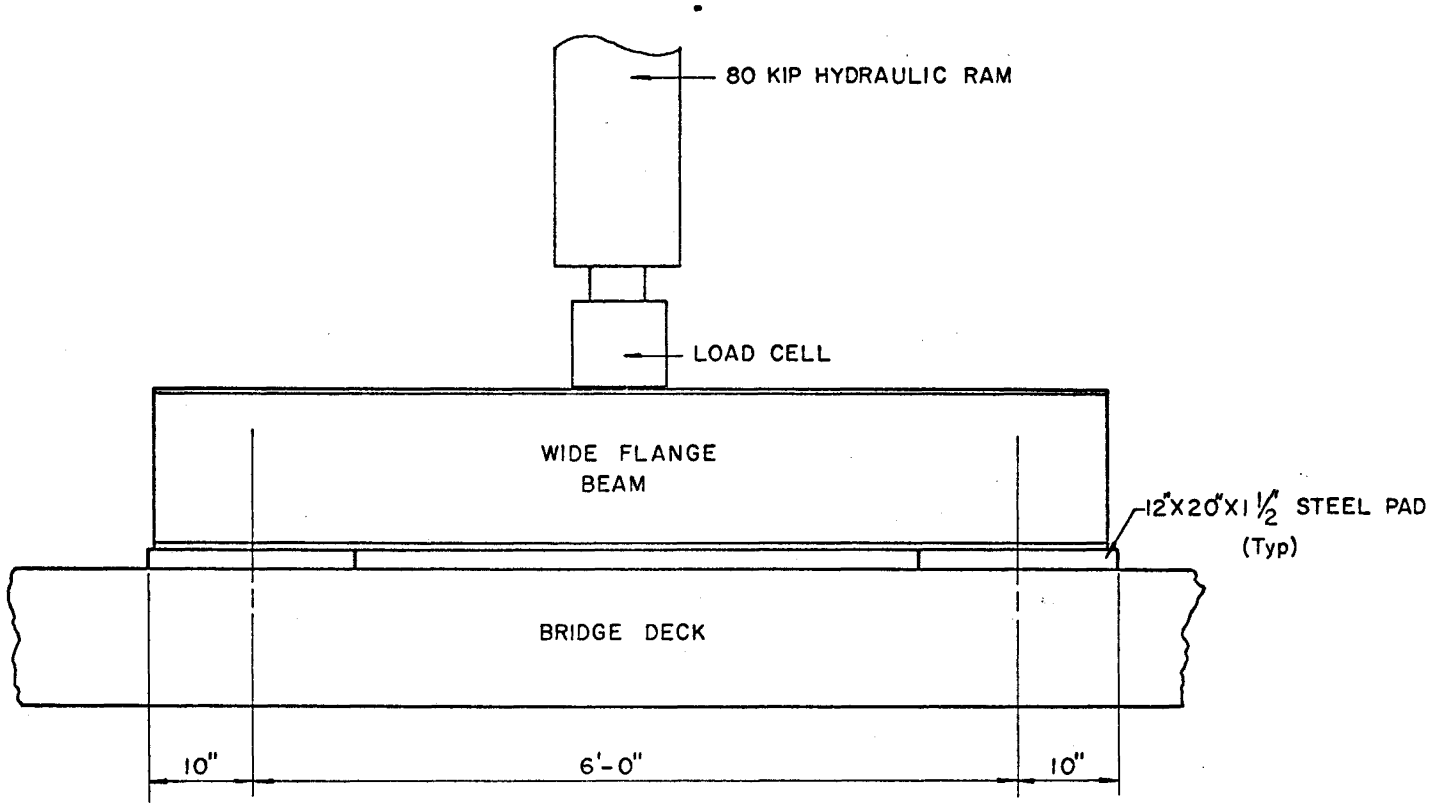

Figure 27. System for applying axle loads to full-scale bridge.

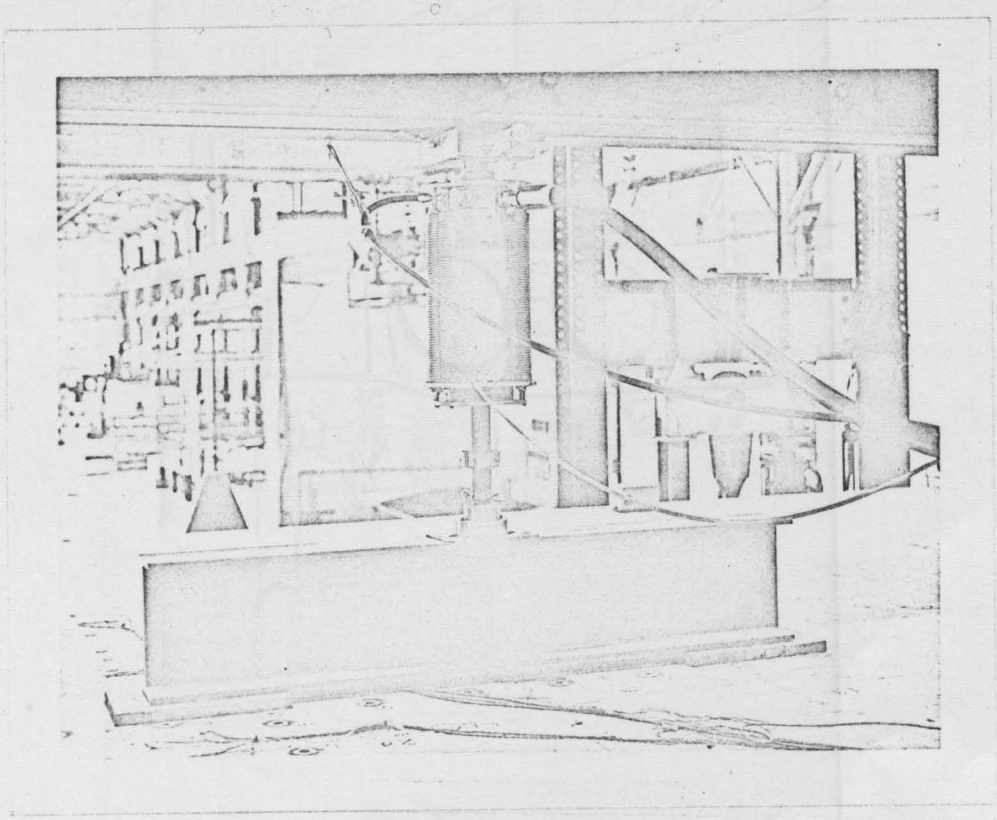

Figure 28. Hydraulic ram and loading pad arrangement for applying axle loads.

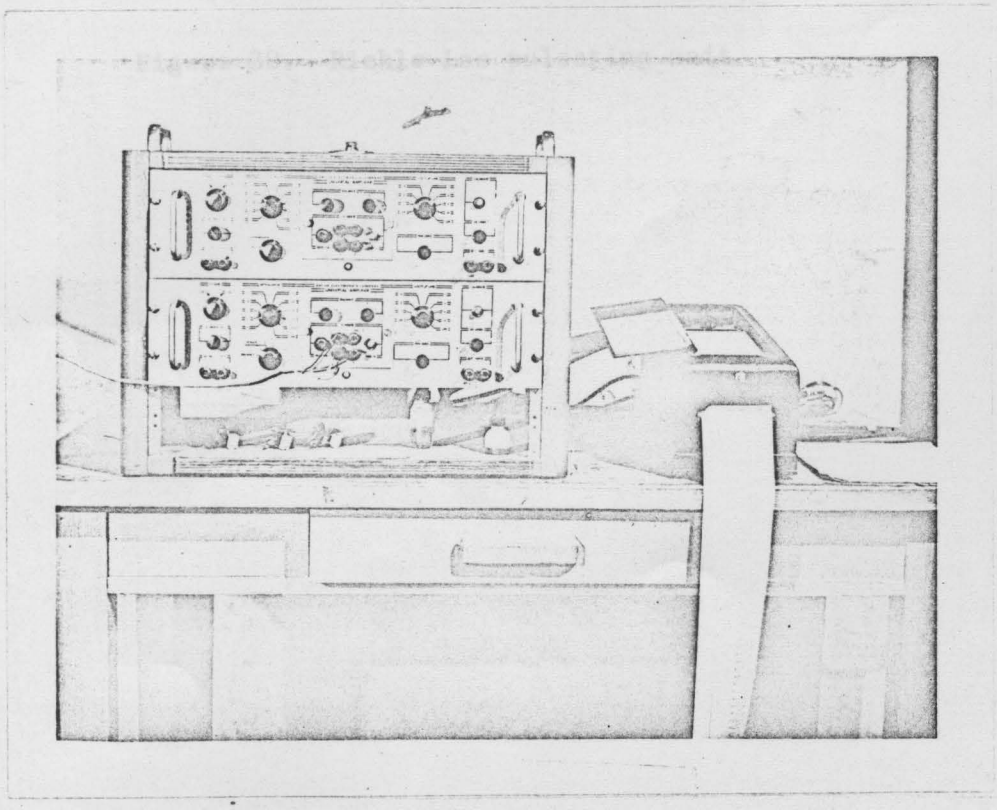

Figure 29. Amplifier and recorder used for measuring load.

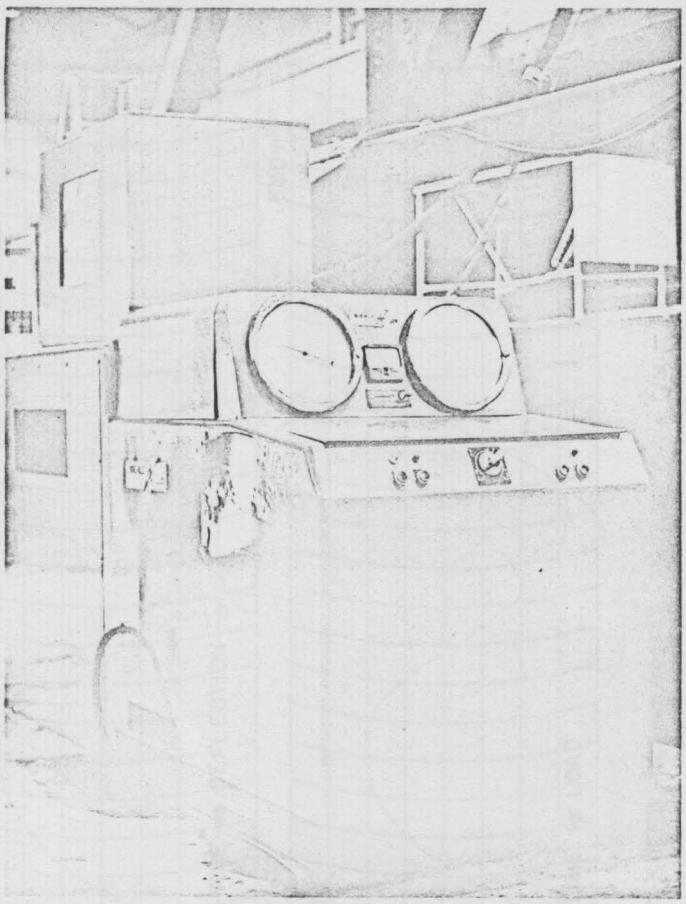

Figure 30. Riehle-Los pulsating unit.

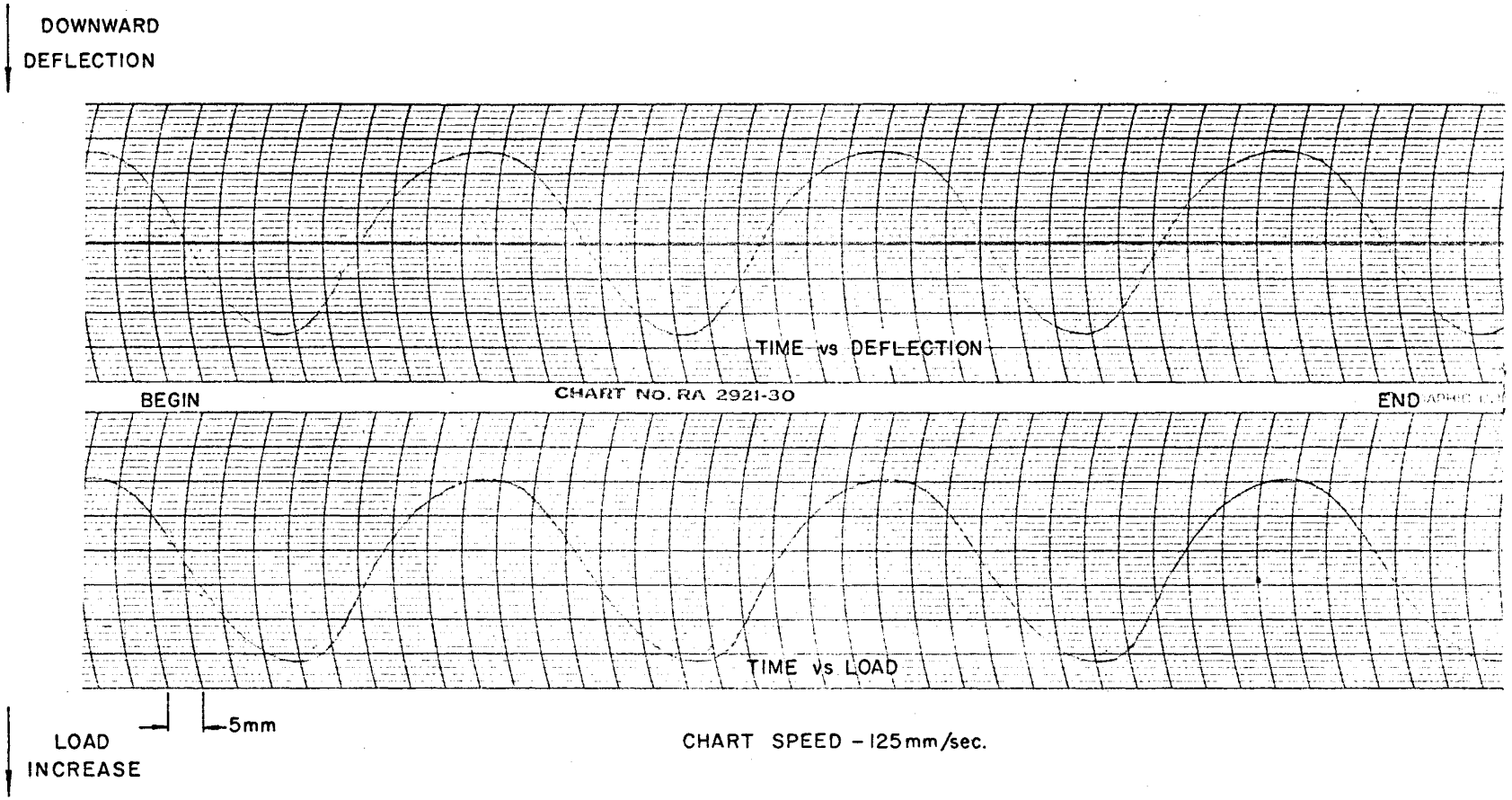

Figure 31. Strip chart record of load and deflection recorded during application of load no. 3.

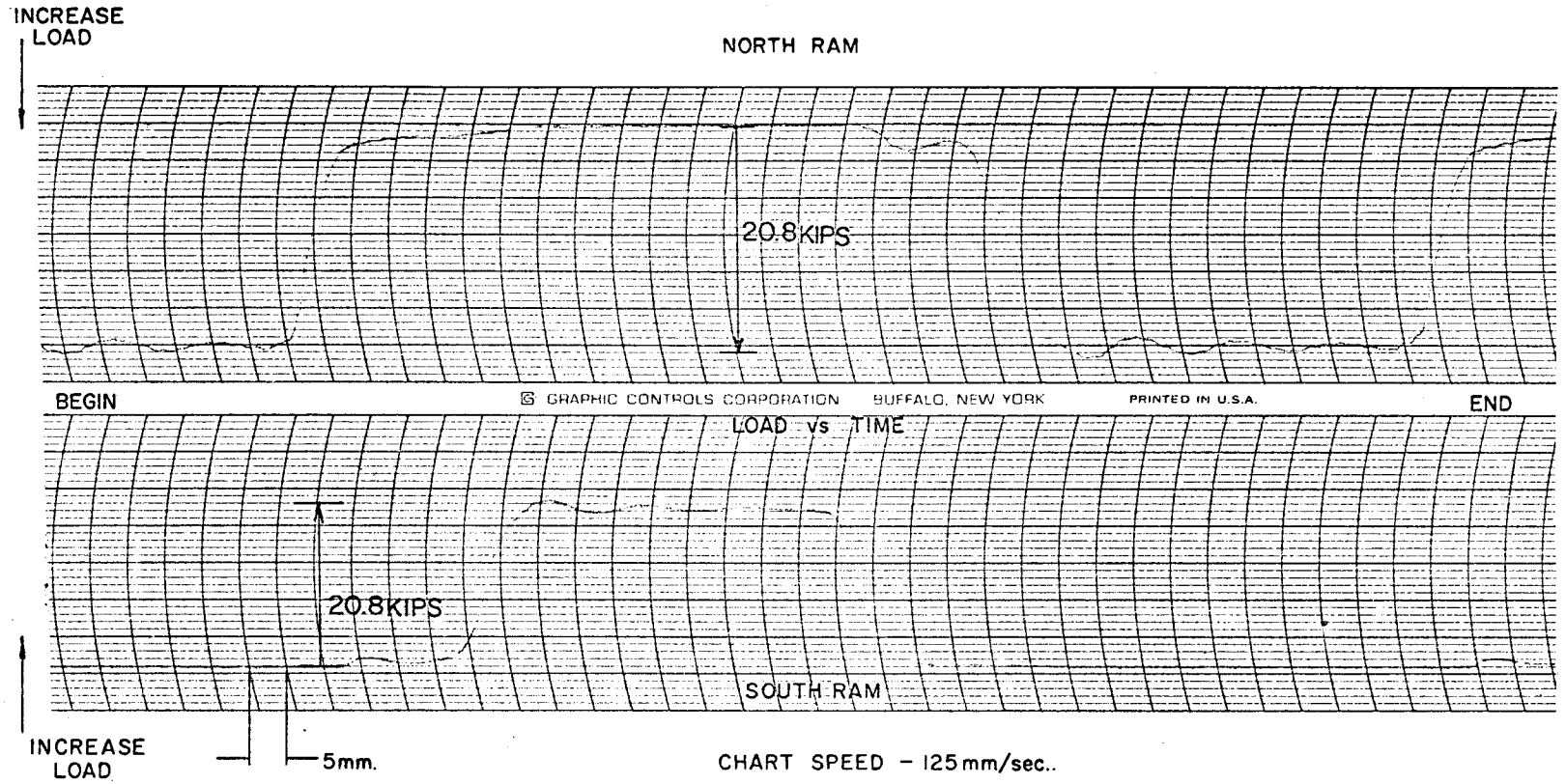

Figure 32. Strip chart record of load vs. time recorded during application of load no. 5.

EXPERIMENTAL PROGRAM

The loading plan, designed to accomplish a complete evaluation of the structure, is listed in Table 2. Loadings 1 through 3 have been accomplished. Loading 5 is in progress but not completed. Loading 4 remains to be conducted and loadings 6, 7 and 8 are each to be applied only in case a failure is experienced under the previous load in each case. Two types of cyclic loads are included in the loading plan. They are axle loads (Nos. 1 through 3) and wheel loads (Nos. 4 through 8). The axle loads are designed to evaluate overall behavior of composite action in the structure. The wheel loads are designed to evaluate the local behavior of the slab at transverse panel butt joints.

The loading plan includes axle loading in an area of Z-bar and dowels, an area of Z-bars with no dowels, and an area with no Z-bars nor dowels. Wheel loadings include loadings at a transverse joint with dowels in a Z-bar area, and at a transverse joint with no dowels in an area of no Z-bars. Further loadings are called for in case of failure at either of these positions.

The general procedure for evaluation of the behavior of the bridge is as follows:

(1) Determine the response of the bridge to a static design load by reading the strains and deflections at all gage locations.

(2) Subject the bridge to a number of cycles of load.

(3) Again determine the response of the bridge to the static load.

(4) Visually inspect the structure each time the static load is applied to determine if any form of distress has occurred.

(5) Compare the responses to static loads obtained in 1 and 3 above to determine if any distress has occurred in the structure.

For loadings 1 through 3, the schedule is: Make "zero" readings on all beam deflection gages, all strain gages, and all deck surface contour gages. Subject the bridge to increments of load of 16 kips up to 48 kips axle load. Read all gages at each load increment. Return to zero load in one step and again read all gages. The structure is visually inspected under zero load and under the full 48 kip axle load. This static load evaluation is conducted before cyclic loading is started, after 1/2 million cycles, after 1 1/2 million cycles and at the end of 2 million cycles.

The design axle load, including 30% increase for impact, was 41.6 kips. The minimum that the cyclic loading equipment is capable of producing on the low end of the load cycle is 8 kips. Therefore, the cyclic axle load ranges from 8 to 49.6 kips and is applied at approximately 160 cycles per minute (2.67 cycles per second). The natural frequency of vibration of the structure was calculated to be 9.2 cycles per second and measured to be 10 cycles per second.

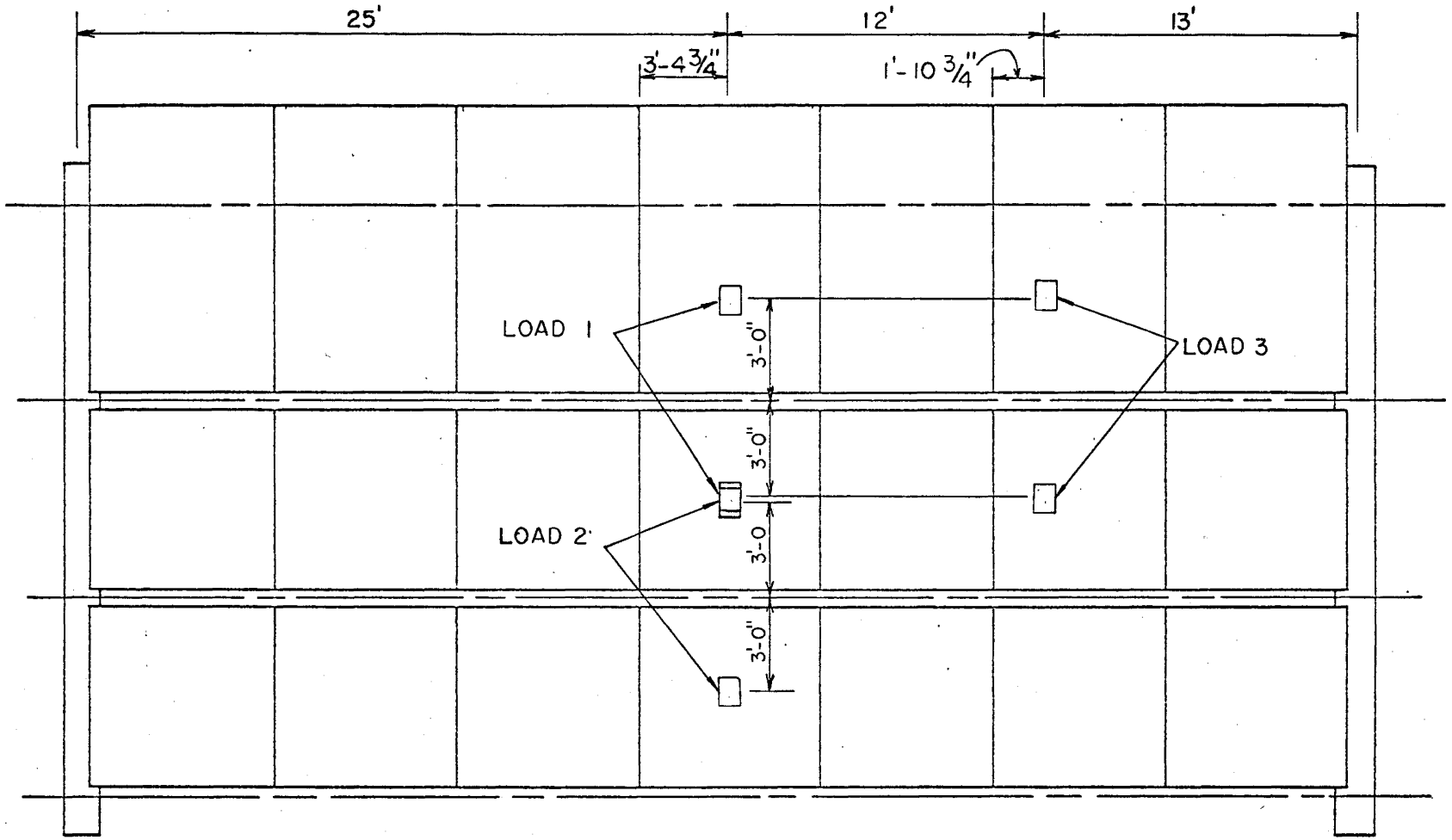

Figure 33. Positions of axle loads.

THEORETICAL CONSIDERATIONS

An elastic analysis procedure has been developed for the bridge model and coded for the digital computer. The analysis assumes the beams and slab to be homogeneous, isotropic and linearly elastic. It includes the effects of in-plane forces in the slab resulting from composite action with the beams, and the additional stiffness imparted to the structure by the torsional rigidity of the beams. The analysis does not take into account the effects of the diaphragms nor the effects of discontinuities in the slab at joints between prestressed panels.

The analysis treats each beam and the segment of slab between each beam as individual elements. Equations have been developed that relate the translational and rotational displacements of each longitudinal edge of a slab to the bending moments, transverse force and in-plane force on the edges. Similar relationships have been developed between moments and forces applied to the upper face of a beam and the resulting displacements there. Equilibrium of forces is then applied to the longitudinal joint between two adjacent slabs and the beam that supports them, and the displacements at the edges of the slab and the top of the beam are then computed. The stresses, strains, bending moments and displacements of any point on the slab or beams can then be computed from the known edge displacements.

An analysis has been run for load positions 1 through 3 to obtain theoretical values of strain and deflection at points on the bridge model where strain and deflection measurements were taken. These theoretical values are compared with measured values taken before and after two million cycles of load in Figures 34 through 39 and Tables 3 through 5.

RESULTS AND DISCUSSION

Plots of beam deflections for loads 1 through 3 before being subjected to cyclic loading and after 2 million cycles of load in each case are presented in Figures 34 through 36. Close comparisons of deflections before cyclic loading with deflections after cyclic loading show that no significant changes were caused by the loading. A close comparison was also obtained between the theoretically computed values of deflection, enclosed in triangles, and experimentally measured values.

Values of measured strain and computed strain for loads 1 through 3 are presented and compared in Tables 3 through 5. The strains can be grouped, on the basis of gage location, into two groups--those adjacent to a panel butt joint and those that are not. Good agreement between theoretical and experimental strains was obtained for gage positions not adjacent to a panel joint. (Compare, for example, the measured and theoretical strain values for gages S-29 & 30 and S-39 & 40 in Table 3, S-49 & 50 and S-59 & 60 in Table 4, and S-69 & 70 and S-79 & 80 in Table 5.) Those transverse gages adjacent to a panel butt joint show somewhat poorer agreement, but with no apparent trends to either overestimate or underestimate the measured values. (See Table 3: S-35 & 36, S-37 & 38, S-41 & 42 and S-43 & 44; Table 4: S-55 & 56, S-57 & 58, S-61 & 62 and S-63 & 64; Table 5: S-75 & 76, S-77 & 78, S-81 & 82 and S-83 & 84.) Longitudinal gages adjacent to butt joints showed the poorest agreement among all gages, with theoretical values being consistently higher than measured ones. This trend is shown in Table 3: gages S-25 & 26, S-27 & 28, S-31 & 32 and S-33 & 34; Table 4: S-45 & 46, S-47 & 48, S-51 & 52 and S-53 & 54; Table 5: S-65 & 66, S-67 & 68,

S-71 & 72 and S-73 & 74. Discrepancies in these readings were expected, since the theoretical solution does not account for panel butt joints. Further consideration is being given to a procedure for modifying the theoretical analysis to include the effects of the butt joints between panels.

Theoretical stresses in the top and bottom of the slab were computed from elastic theory and compared to stresses computed from strains measured by the electrical resistance gages. These stresses were found from the relation:

$$\sigma_x = \frac{E}{1-\nu^2} \quad (\varepsilon_x + \nu\varepsilon_y)$$

The modulus of elasticity E was taken as 5,450,000 psi, which is the average of the modulus values for prestressed panel and cast-in-place deck. Poisson's ratio ν, was assumed to be 0.16. Stresses calculated from strains measured both before and after cyclic loading for loadings 1 through 3 and theoretically predicted stresses are presented in Figures 37 through 39. Strains from adjacent longitudinal and transverse gages were assumed to be at the same point for purposes of these calculations, although points of strain are separated by approximately 3 inches (Figure 20). The strain gradient in the slab near the gages is not great enough to cause any appreciable error by this assumption.

It is observed that all stresses are small in magnitude. The largest measured tensile stress which occurred on the bottom of a prestressed panel adjacent to a wheel load was 436 psi. A compressive prestress plus dead-load stress of 497 psi was computed to exist at that point. This results in a net stress of 61 psi compression. Slightly larger stresses due to load

exist directly under the wheel load pad. In the design of the bridge, it was intended that a zero net stress would exist at that point. In all cases except at the panel butt joint nearest the east wheel pad of loading 3, the stresses in the longitudinal direction of the bridge on the bottom side of the panel at the panel butt joints were compressive stresses.

The agreement between theoretical and experimental stresses is not as close as desired in all cases, but in most cases it is good. Further work is being conducted to attempt to obtain closer agreement between them.

Prior to application of load 3, minute cracks, 0.002 inches in width, were discovered above some transverse joints between panels. These cracks were not found upon inspection after conclusion of load 2. Some cracks were in the vicinity of a panel joint near the north end of the bridge, far removed from the loads and it is believed that they are due to shrinkage or thermal strains, or both, and not due to load. A pattern of these cracks is presented in Figure 40.

TABLE 3

Experimental and Theoretical Strains for Load Position 1

Axle Load of 48 kips

Strain Gage	Experimental Strain, μ in/in		Theoretical Strain μ in/in
	Before Cyclic Loading	After Cyclic Loading	
S-25	-11	-15	-27
S-26	-26	-17	-28
S-27	-14	-13	-22
S-28	-20	-14	-34
S-29	-56	-56	-56
S-30	+ 1	- 2	- 2
S-31	-16	-14	-22
S-32	-19	-15	-34
S-33	-15	-14	-27
S-34	-16	-13	-28
S-35	-18	-23	-24
S-36	+14	+26	+31
S-37	-39	-27	-29
S-38	+20	+33	+37
S-39	-74	-76	-65
S-40	+61	+74	+71
S-41	-28	-24	-29
S-42	+25	+36	+37
S-43	-39	-38	-24
S-44	+18	+24	+31

TABLE 4

Experimental and Theoretical Strains for Load Position 2

Axle Load of 48 kips

Strain Gage	Experimental Strain, μ in/in		Theoretical Strain μ in/in
	Before Cyclic Loading	After Cyclic Loading	
S-45	- 9	- 5	-18
S-46	-15	-14	-21
S-47	- 3	- 4	-13
S-48	-17	-14	-27
S-49	-32	-32	-46
S-50	+ 7	+ 1	+ 5
S-51	- 7	- 7	-13
S-52	-23	-19	-27
S-53	-23	-24	-18
S-54	-23	-19	-21
S-55	-21	-21	-23
S-56	+22	+24	+30
S-57	-31	-27	-28
S-58	+47	+34	+35
S-59	-77	-62	-63
S-60	+75	+76	+69
S-61	-32	-29	-28
S-62	+31	+36	+35
S-63	-11	-12	-23
S-64	+25		+30

TABLE 5

Experimental and Theoretical Strains for Load Position 3

Axle Load of 48 kips

Strain Gage	Experimental Strain, μ in/in		Theoretical Strain μ in/in
	Before Cyclic Loading	After Cyclic Loading	
S-65	- 4	-10	-17
S-66	- 8	-14	-11
S-67	- 6	-11	-17
S-68	-10	-18	-13
S-69	-12	-18	-34
S-70	-13	-21	- 5
S-71	-13	-18	-36
S-72	- 3	-20	- 8
S-73	-16	-25	-20
S-74	+ 3	+ 3	-24
S-75	- 7	-14	-11
S-76	+13	+ 9	+16
S-77	-12	-20	-14
S-78	+17	+13	+19
S-79	-52	-59	-54
S-80	+53	+51	+58
S-81	-50	-58	-54
S-82	+66	+56	+58
S-83	-54	-57	-40
S-84	+50	+40	+45

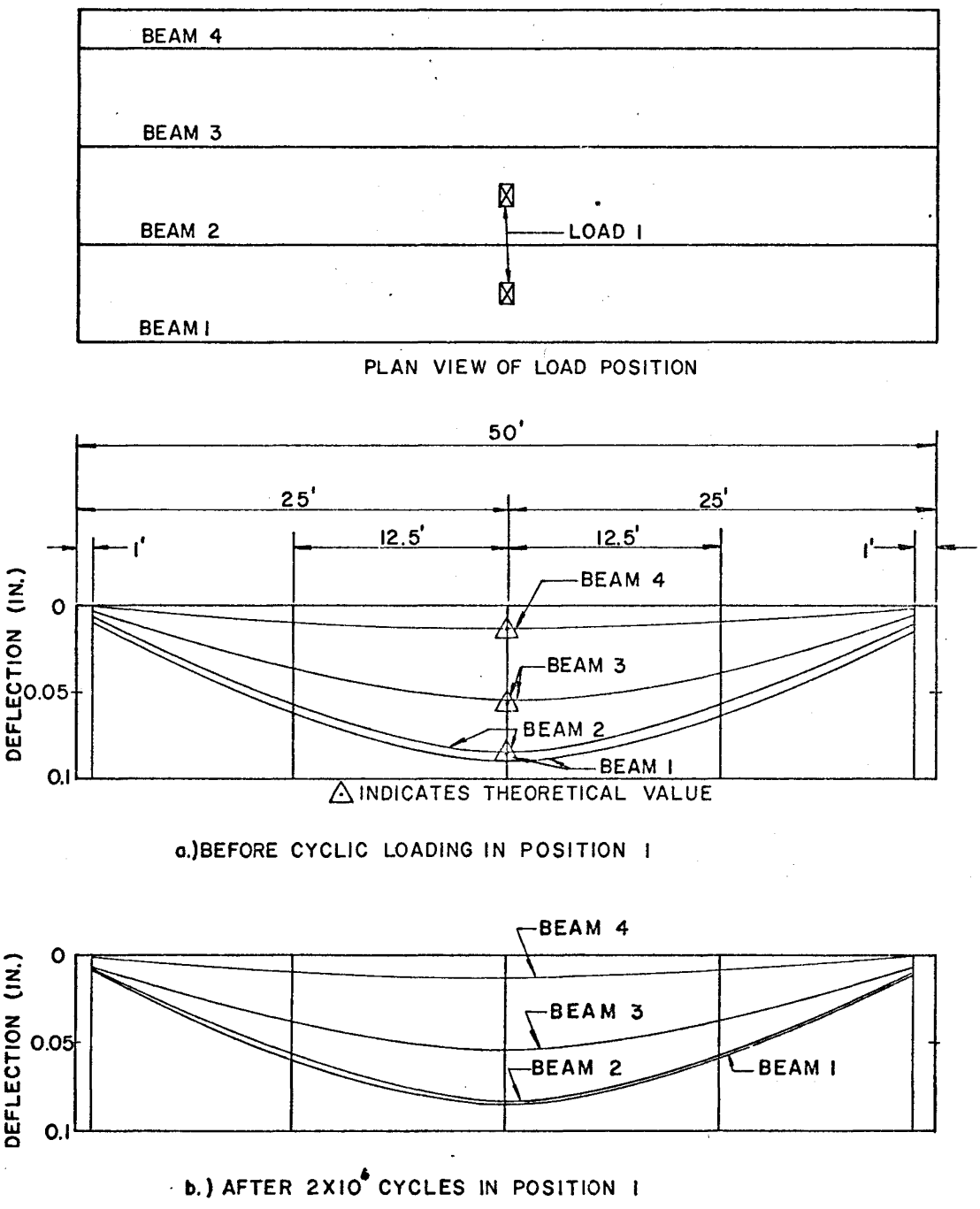

Fig. 34. Theoretical and experimental beam deflections for loading 1.

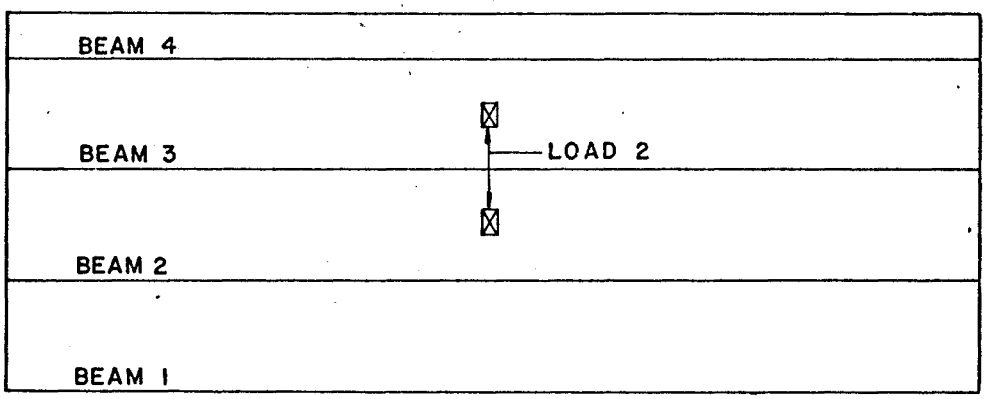

PLAN VIEW OF LOAD POSITION

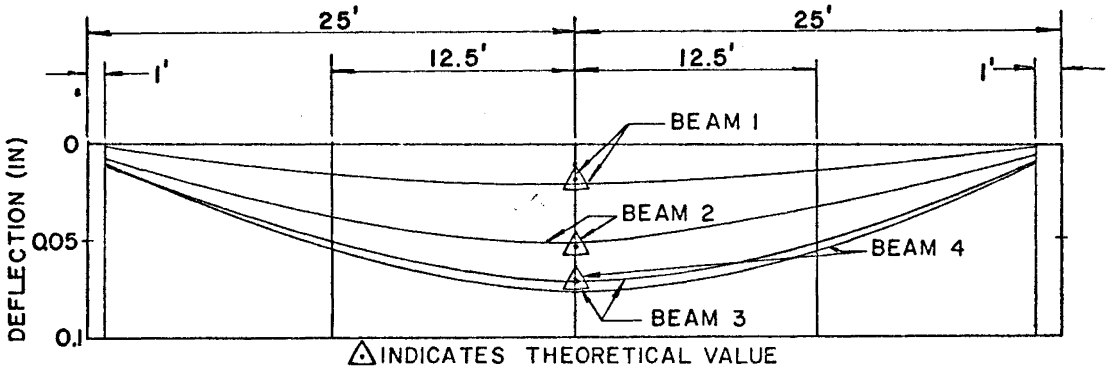

a.) BEFORE CYCLIC LOADING IN POSITION 2

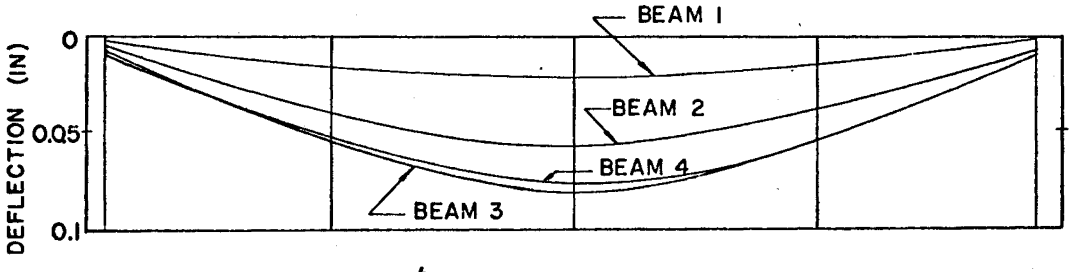

b.) AFTER 2×10^6 CYCLES IN POSITION 2

Fig. 35. Theoretical and experimental beam deflections for loading 2.

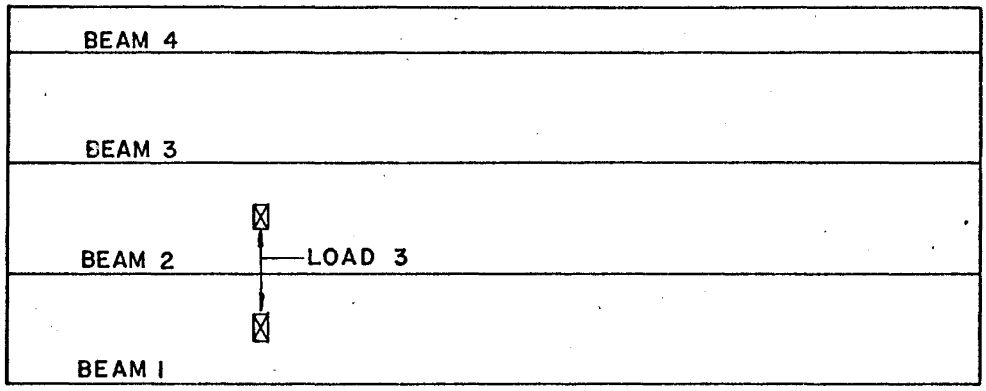

PLAN VIEW OF LOAD POSITION

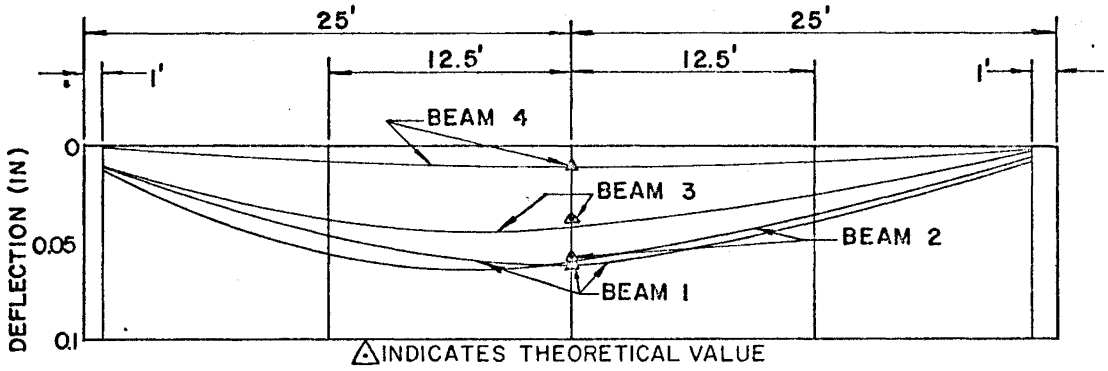

a.)BEFORE CYCLIC LOADING IN POSITION 3

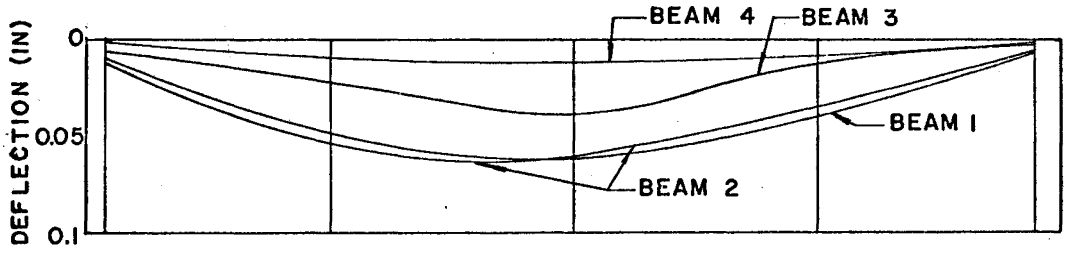

b.) AFTER 2×10^6 CYCLES IN POSITION 3

Fig. 36. Theoretical and experimental beam deflections for loading 3.

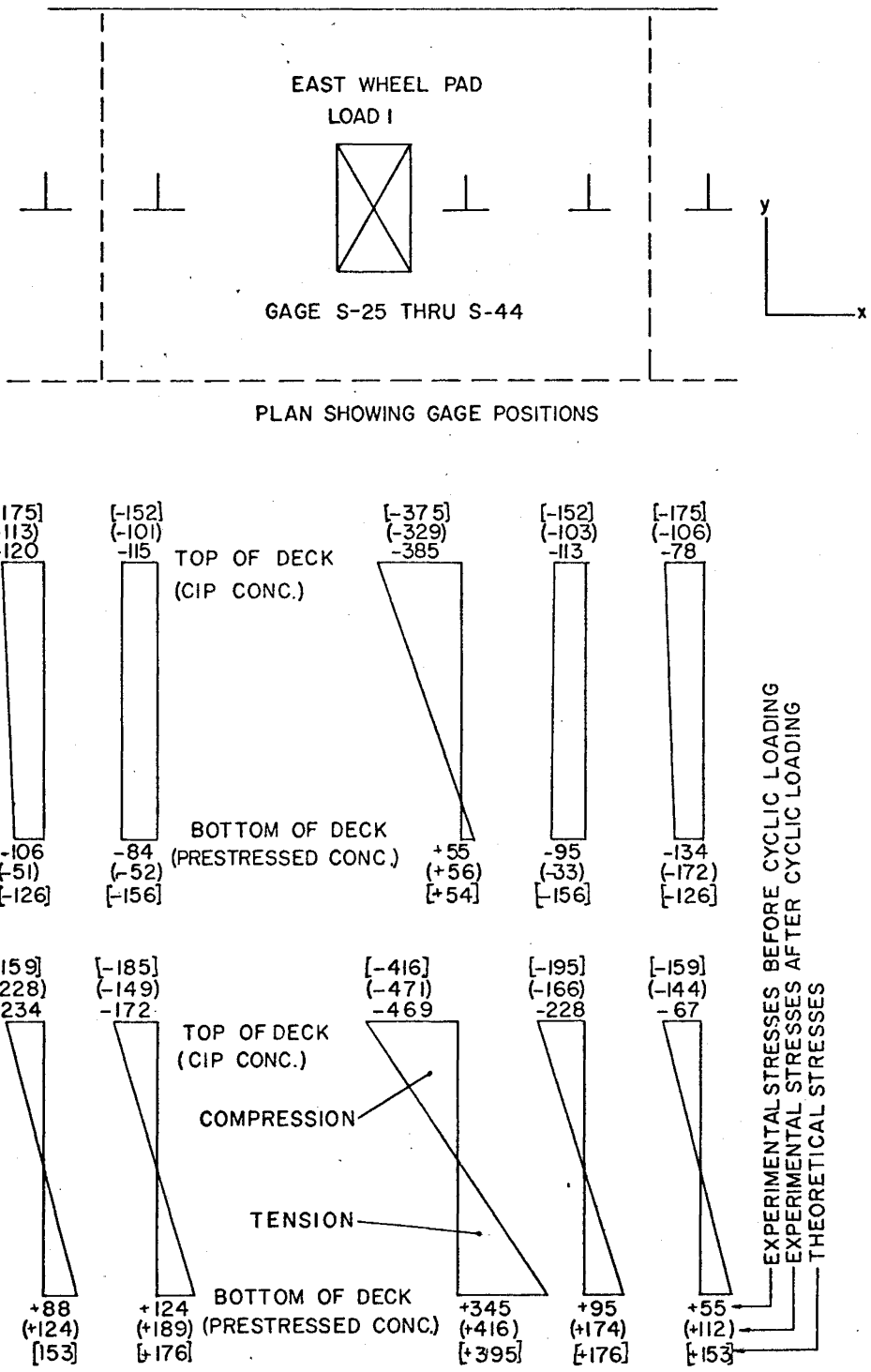

Figure 37. Stress diagrams showing experimental and theoretical stresses at selected locations for loading no. 1.

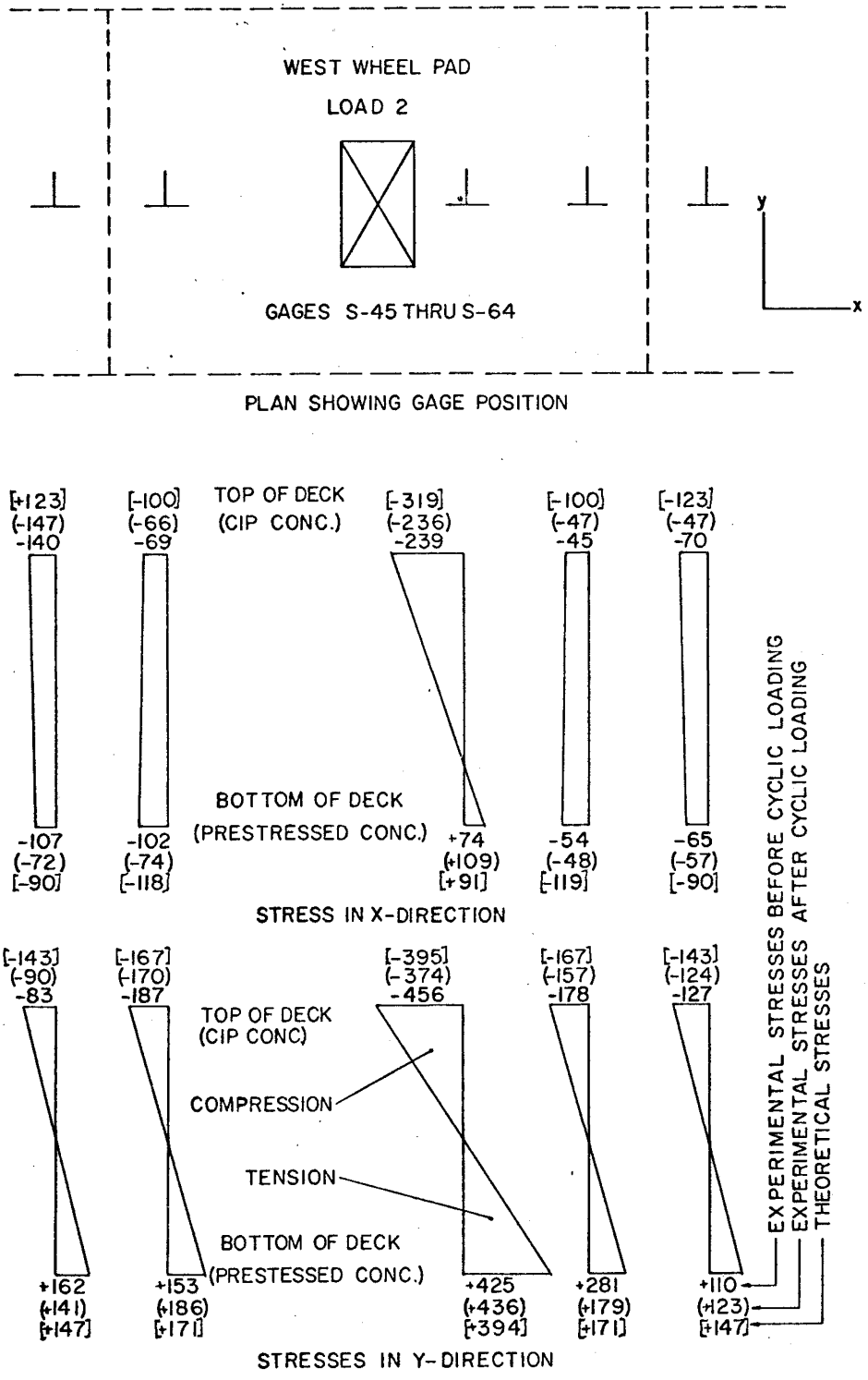

Figure 38. Stress diagrams showing experimental and theoretical stresses at selected locations for loading no. 2.

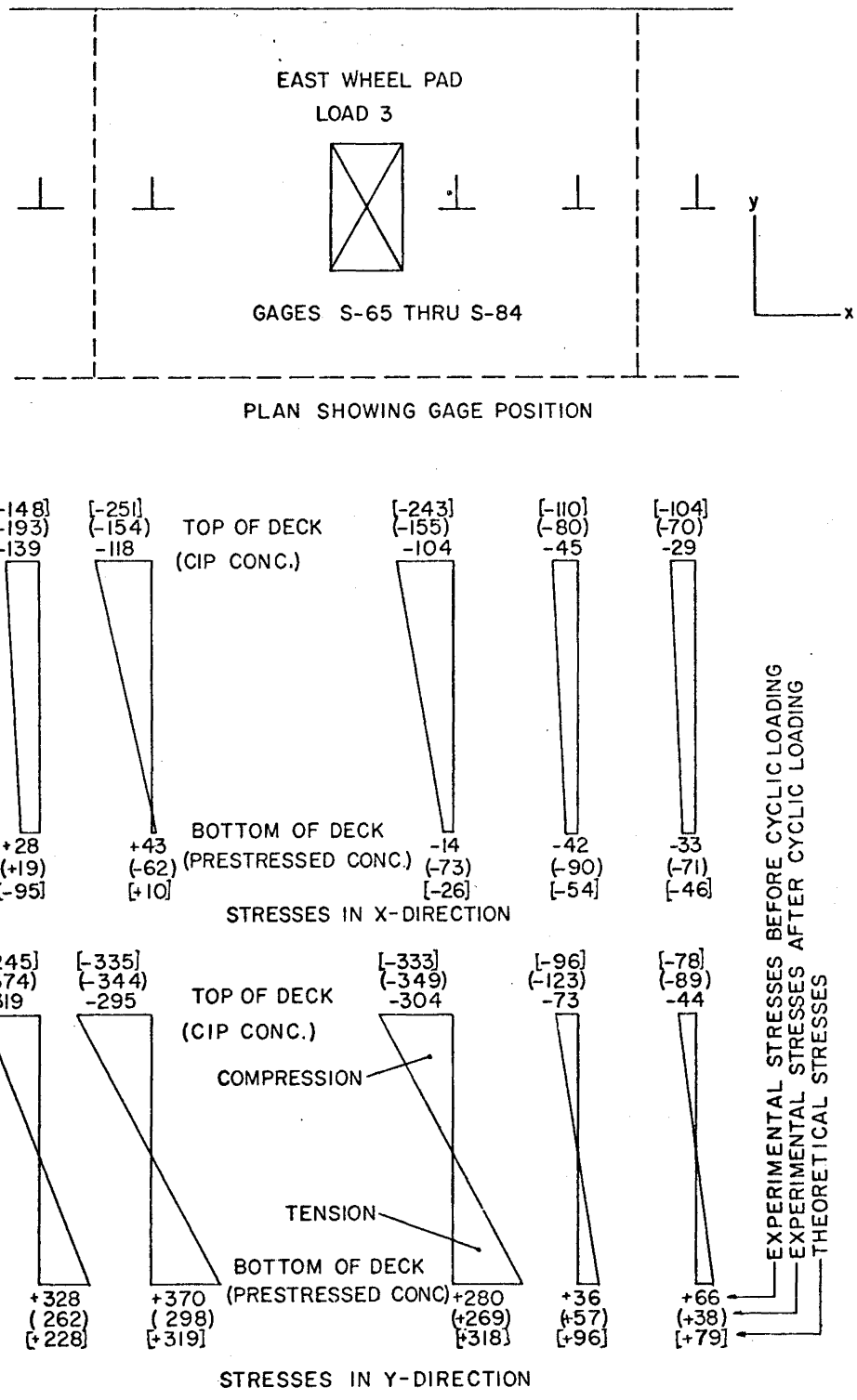

Figure 39. Stress diagrams showing experimental and theoretical stresses at selected locations for loading no. 3.

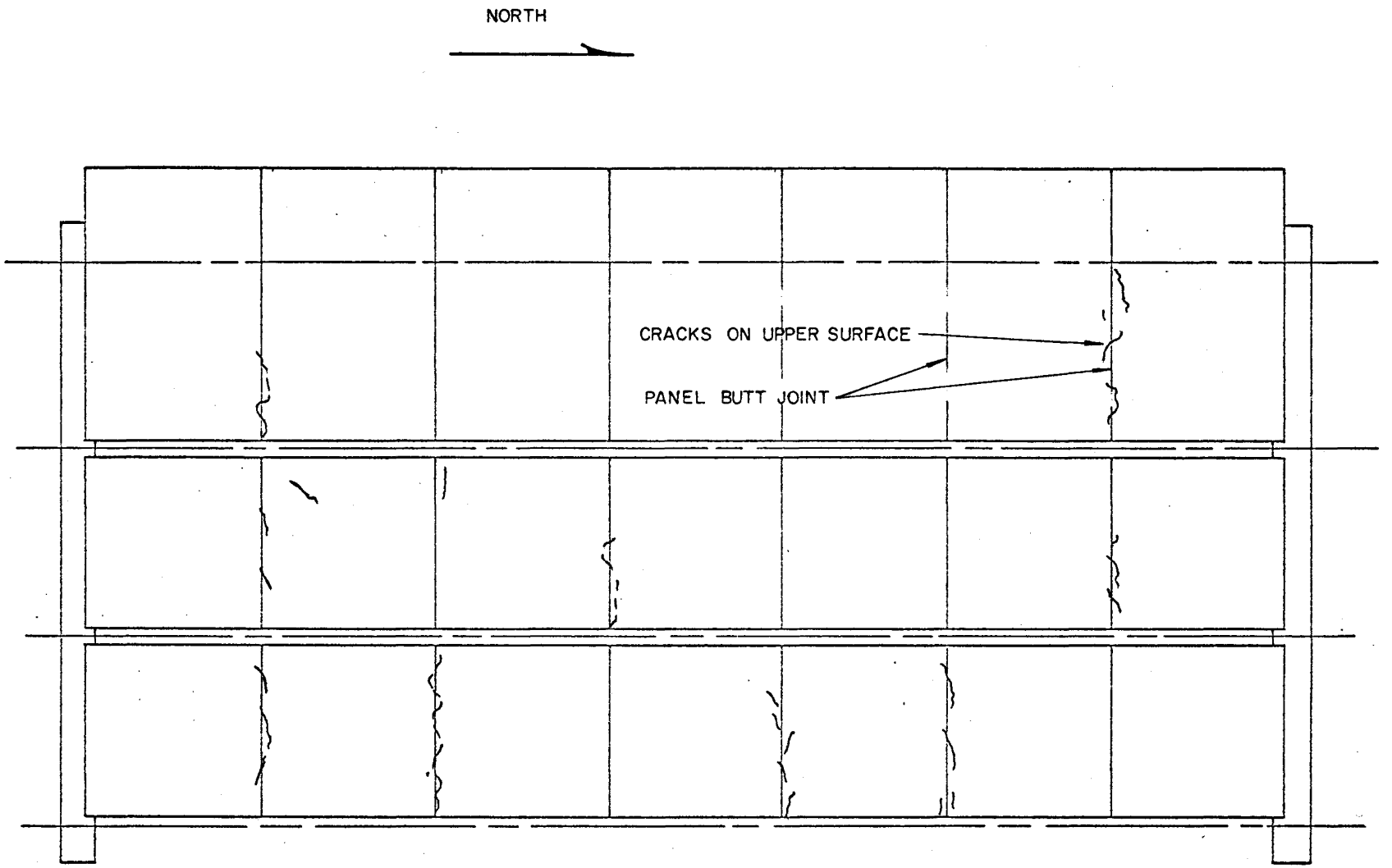

Figure 40. Map of Cracking Pattern.

SUMMARY

Two million applications of axle load have been applied at load positions 1 through 3. No structural distress has been created by these loads. The response of the structure to static loads in each of the 3 positions as measured by beam deflections, slab strains, and visual observation was the same after cyclic loading as it was before cyclic loading. Theoretically predicted beam deflections compare closely with those measured experimentally. Theoretically predicted strains and stresses in the deck compare well with those obtained from experimental data except for gage positions near panel butt joints. The theoretical solution does not account for panel butt joints. No slip or differential movement was detected between the prestressed panels and prestressed beams or between the prestressed panels and cast-in-place deck.

REFERENCES

1. Ingram, Leonard L., and Butler, H. D., "Prestressed Concrete Bridge Girder Design Program", Research Report 149-1, Texas Transportation Institute, Texas A&M University, College Station, Texas, November 1970.

2. Jones, Harry L., and Furr, Howard L., "Study of In-service Bridges Constructed with Prestressed Panel Sub-decks", Research Report 145-1, Texas Transportation Institute, Texas A&M University, College Station, Texas, July 1970.

3. Jones, H. L., and Furr, H. L., "Development Length of Strands in Prestressed Panel Subdecks", Research Report 145-2, Texas Transportation Institute, Texas A&M University, December 1970.

4. Standard Specifications for Highway Bridges, Tenth Edition, American Association of State Highway Officials, Washington, D.C., 1969.

5. ASTM Standard Specifications for Concrete and Mineral Aggregates, American Society for Testing and Materials, Philadelphia, Pennsylvania.